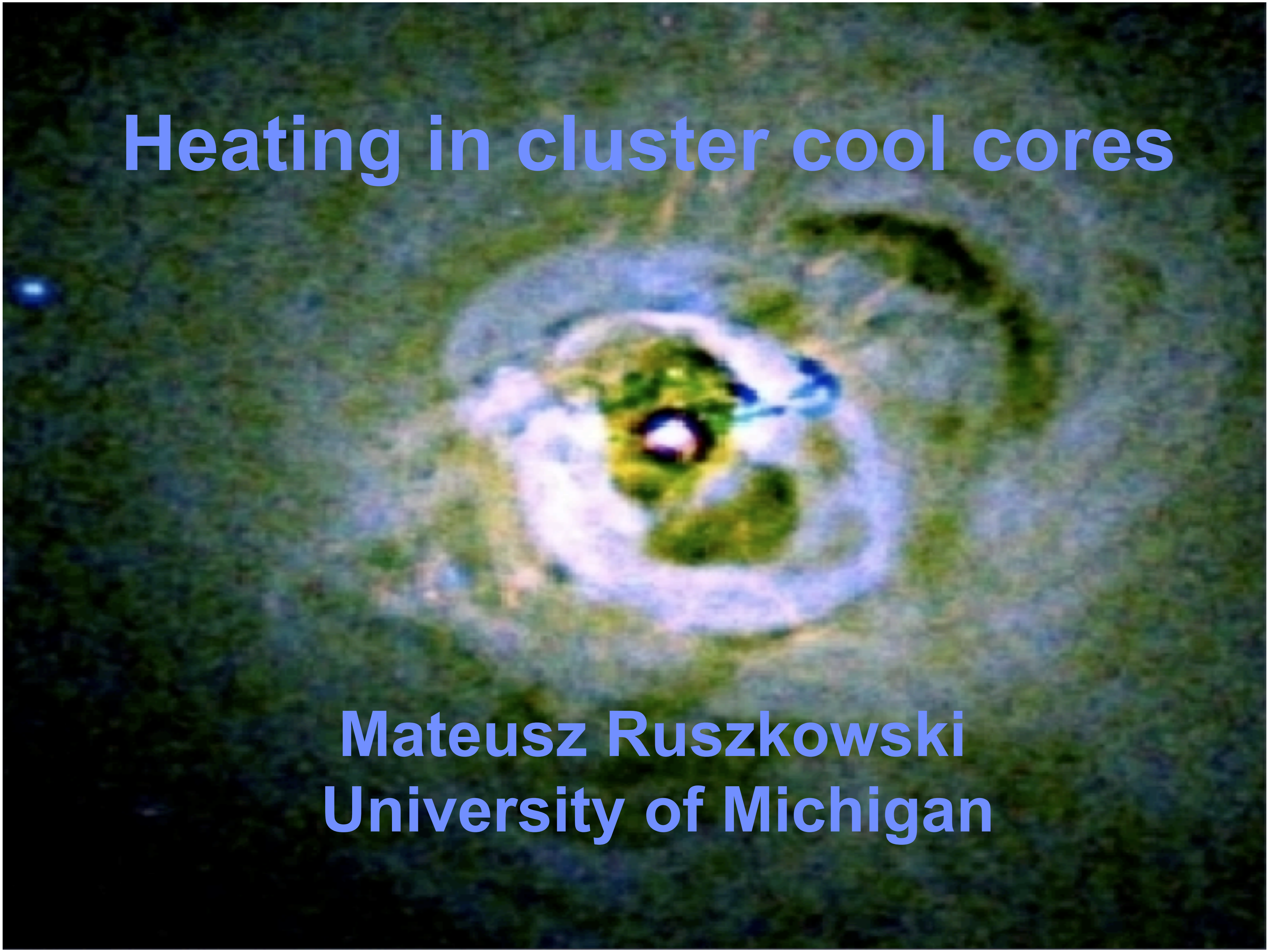

Heating in cluster cool cores

Mateusz Ruszkowski
University of Michigan

People (on the papers discussed in this talk):

Peng Oh
Fulai Guo
Alexis Finoguenov
Christine Jones
Alexey Vikhlinin
E. Mandell
Ian Parrish
Torsten Ensslin
Marcus Bruggen
Mitch Begelman
Christoph Pfrommer
Sebastian Heinz
Eugene Churazov

Outline

Global stability of heated cool cores

Reality check: observations of M84 an excuse to study: bubbles, waves, CR and their escape

Stability of magnetized bubbles

Escape of non-thermal particles from bubbles into the ICM

Escape of CR from cool cores and convective stability

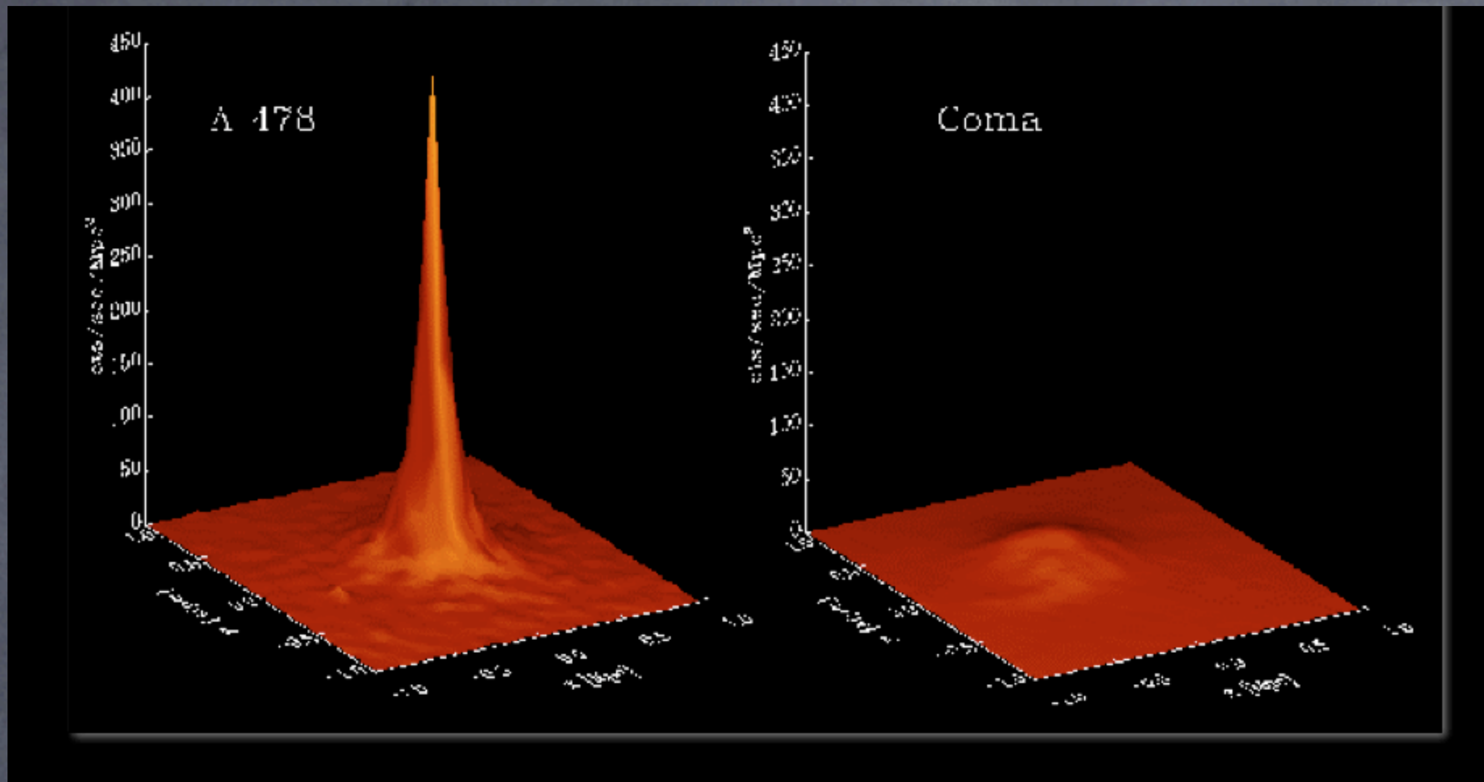

cool core cluster non-cool core cluster

50-70% of clusters have cool cores

Semi-analytical approach:

- ✓ $\boxed{\infty}$ resolution !!
- ✓ easy to search the parameter space
- ✓ better physical insight

Strongly destabilizing

$$C = n^2 \Lambda(T) \propto n^2 T^{\alpha}$$

$$-\nabla \cdot F = \nabla \cdot (\kappa \nabla T)$$

stabilizing

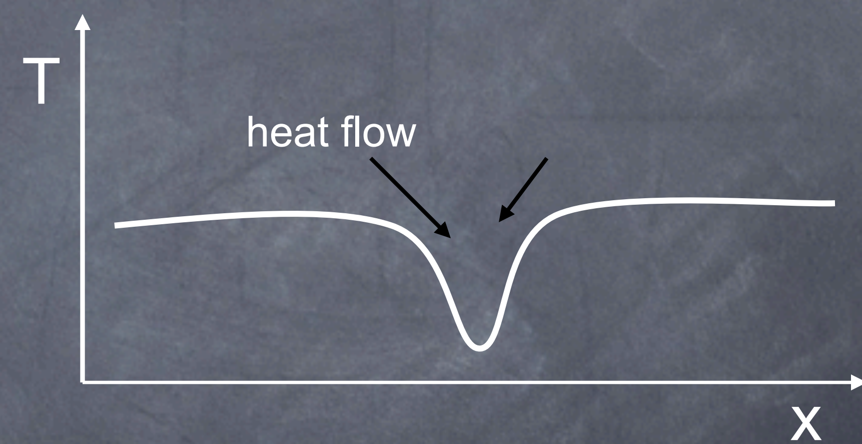

$$H \sim -\nabla \cdot F_{mech} \propto \dot{M}\,\frac{p^{1/4}}{r^3}\,\frac{d\ln p}{d\ln r}$$

spatial heating profile less important than the feedback itself

stabilizing

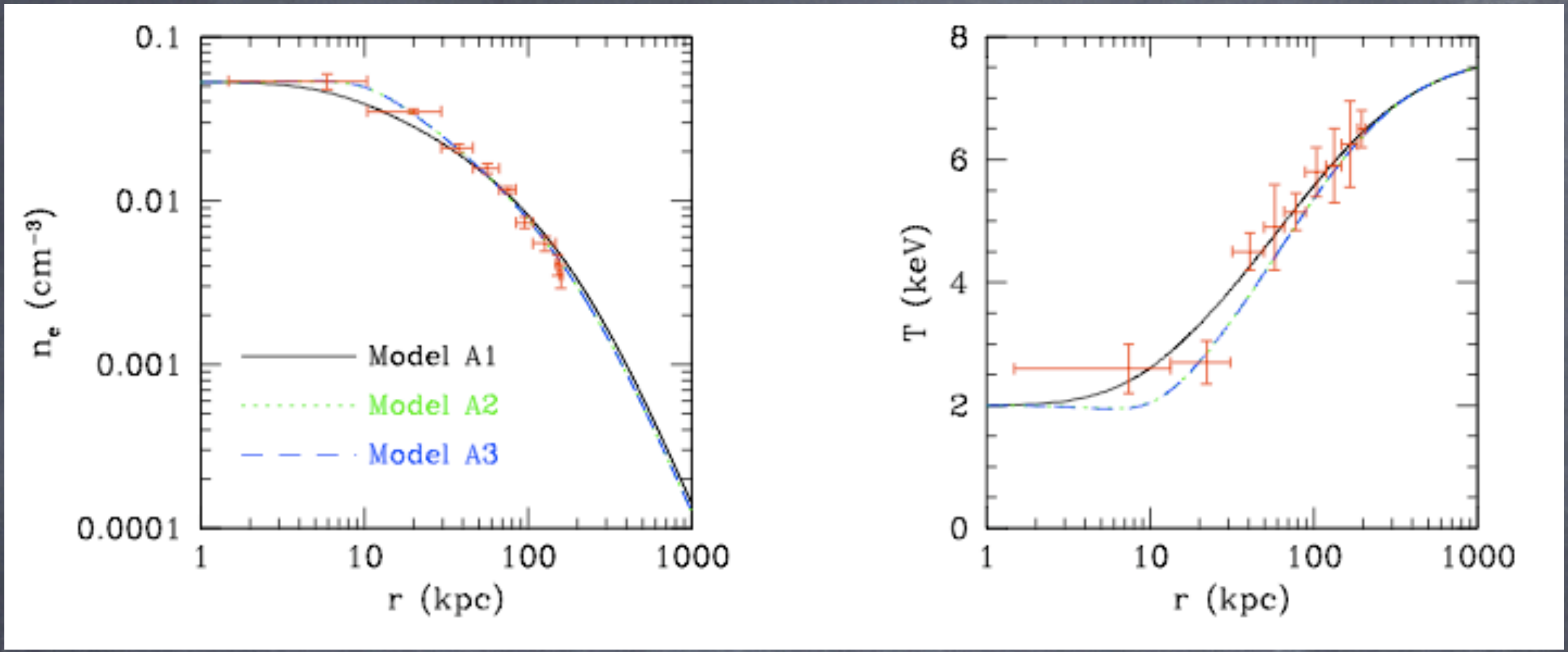

Background model fits the data

We want to study the <u>whole range cluster parameters</u>, so …

- ✓ take background profiles
- ✓ apply Lagrangian perturbations and linearize the hydro equations
- ✓ study all growing (unstable) and decaying (stable) solutions

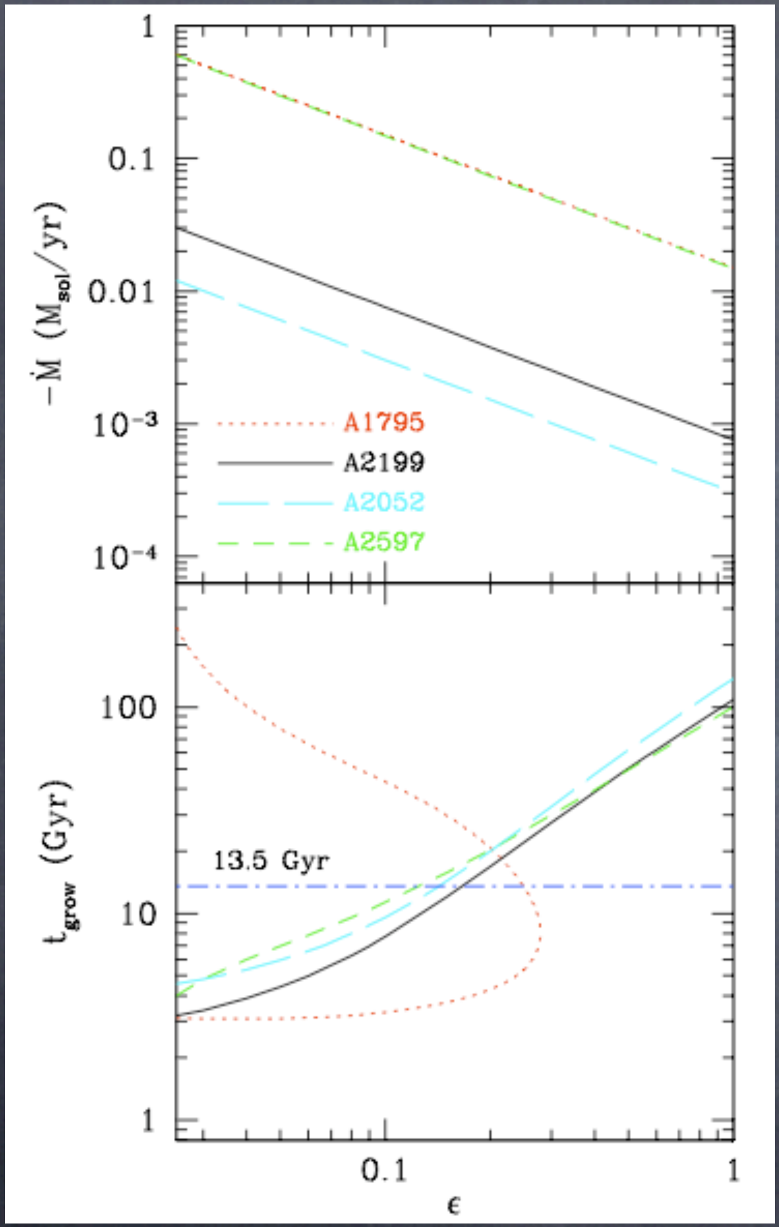

Guo, Oh & Ruszkowski 2008

low accretion rates

$$L_{agn} = -\varepsilon \dot{M} c^2$$

✓ efficiency threshold for stability

✓ efficiencies agree with

Allen et al. 2006

Merloni & Heinz 2007

Churazov et al. 2001

Guo, Oh & Ruszkowski 2008

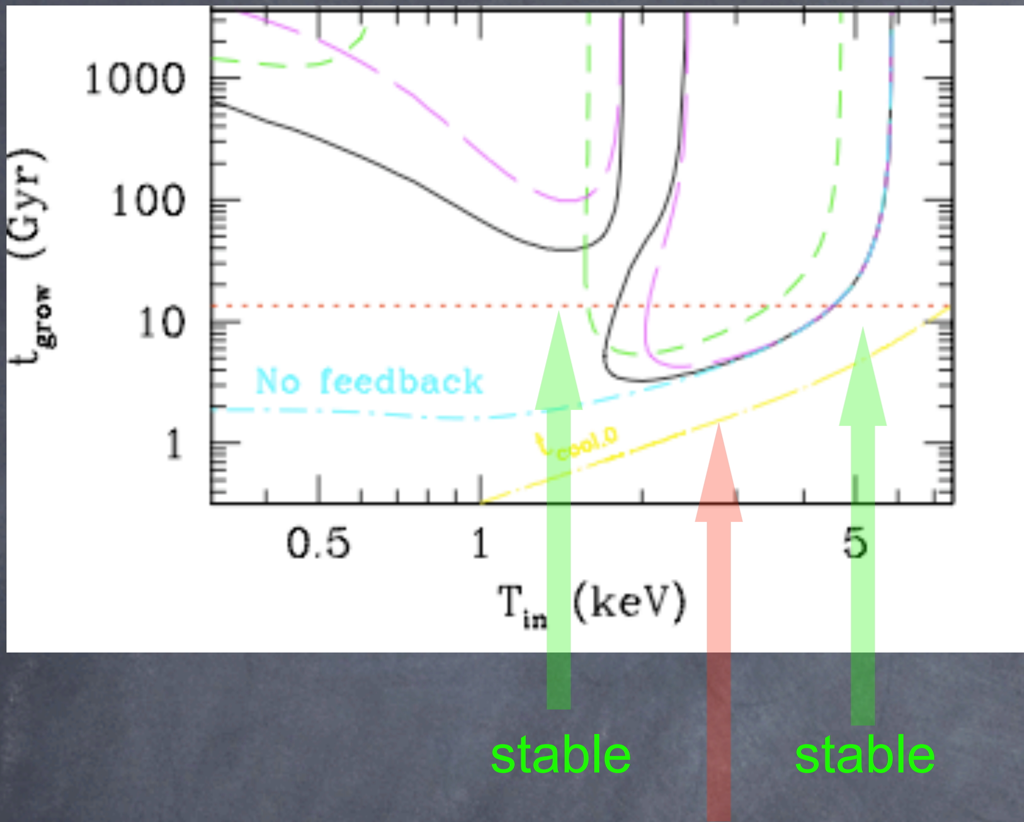

Two diagrams

Bimodality !

cool core ⟵ stabilized by AGN + conduction

non cool core ⟵ stabilized by conduction hint for bimodality

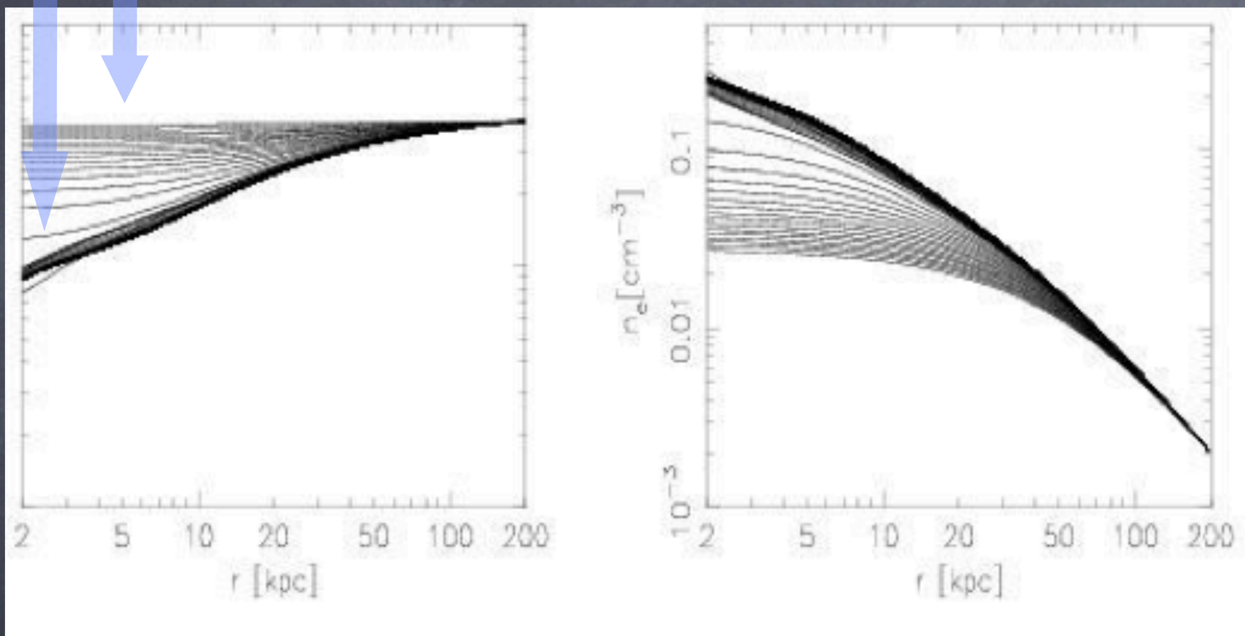

Ruszkowski & Begelman 2002

Trends seen in the data

Dunn & Fabian 2008

AGN on
low central T
low central entropy
short central cooling time

AGN off
high central T
High central entropy
Long central cooling time

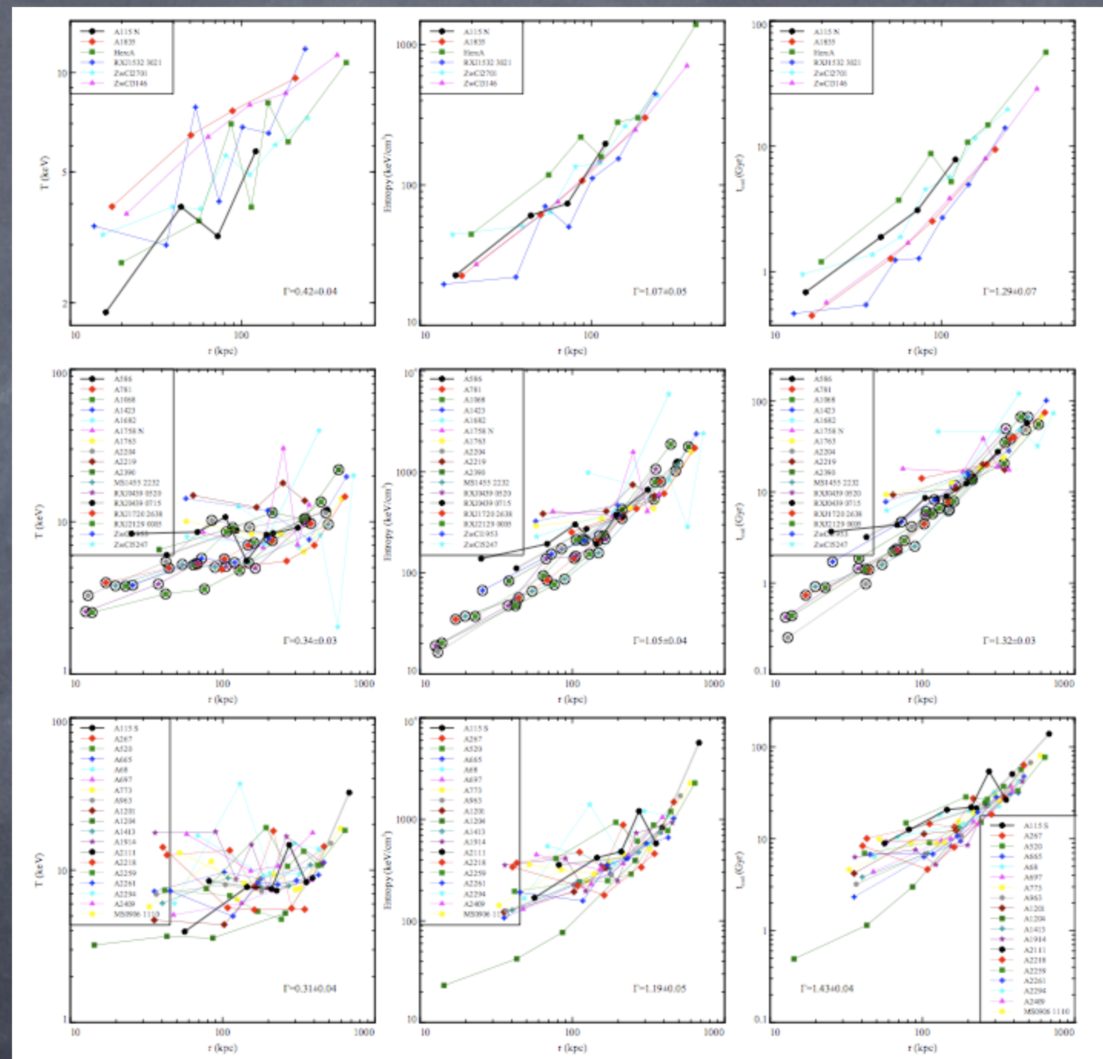

Rafferty et al. 2008

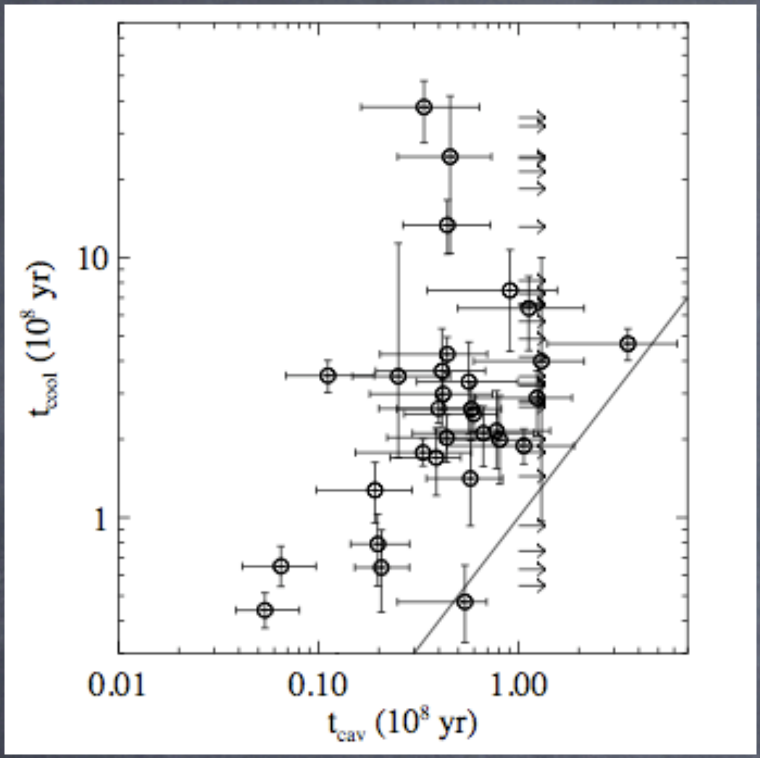

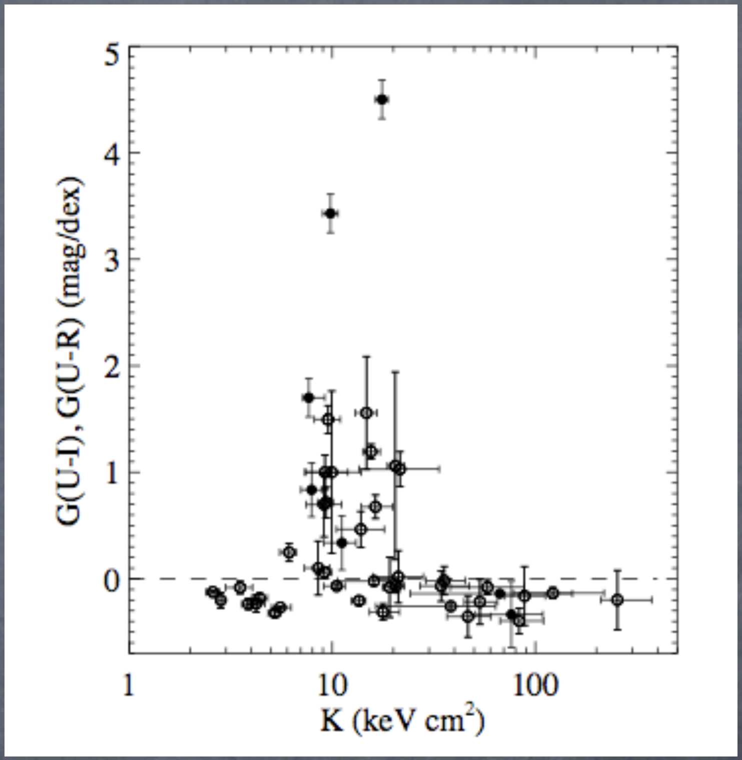

Short central cooling time → Young AGN bubbles

Low central entropy → Star formation & AGN feeding

See also Mark Voit's talk on the effects of conduction on AGN feeding

- ✓ The model is broadly **consistent** with the data
- ✓ Shown for the first time that AGN + conduction can heat the cool cores across a range of cluster parameters in a **stable** fashion
- ✓ The model naturally explains why clusters come in **cool core** and **non-cool core** varieties

Reality check - **AGN feedback in M84** as an excellent lab

- ✓ Bubbles
- ✓ Waves
- ✓ Escape of cosmic rays from the bubbles
- ✓ ISM “weather”

Finoguenov, Ruszkowski, Jones, Bruggen, Vikhlinin, Mandell 2008

Deep ~ **100 000** second *Chandra* observation of M84

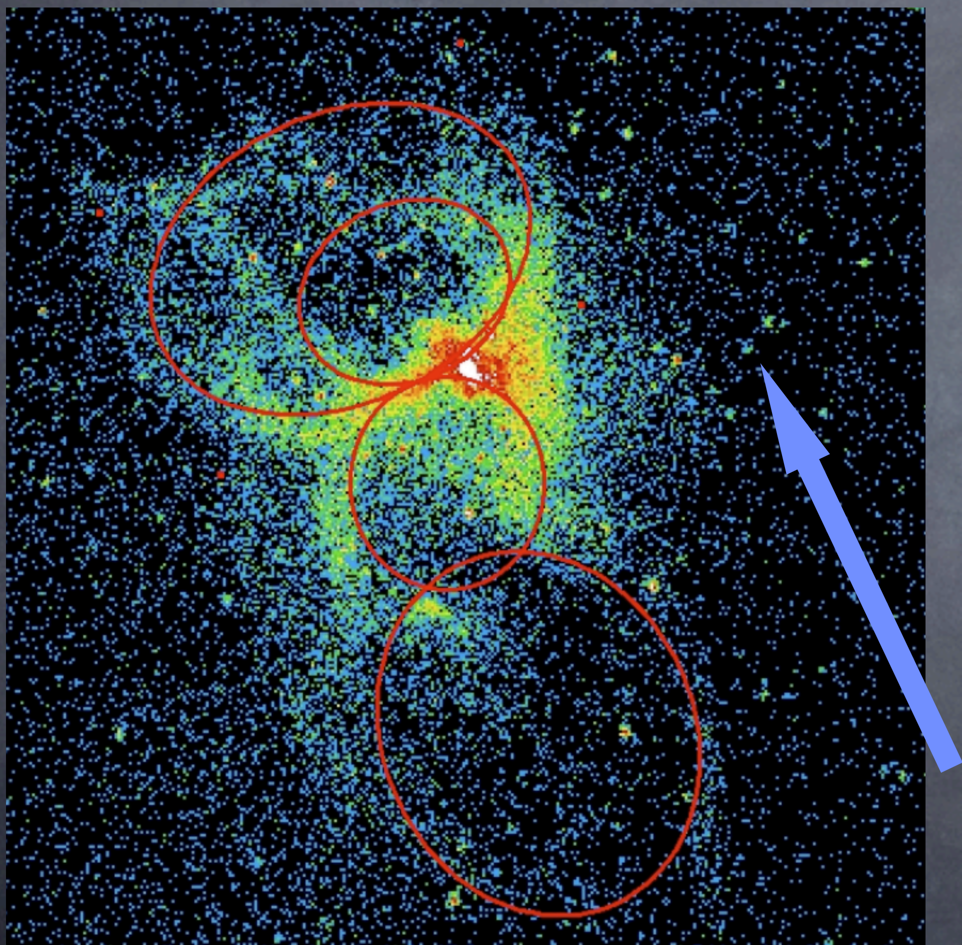

Russian doll X-ray cavities

relative motion of the AGN with respect to the ISM (distorted cavities)

direction of M84 motion (speed comparable to cavity expansion velocity)

Non-thermal particles (cosmic rays)
escape and “pollute” the ISM

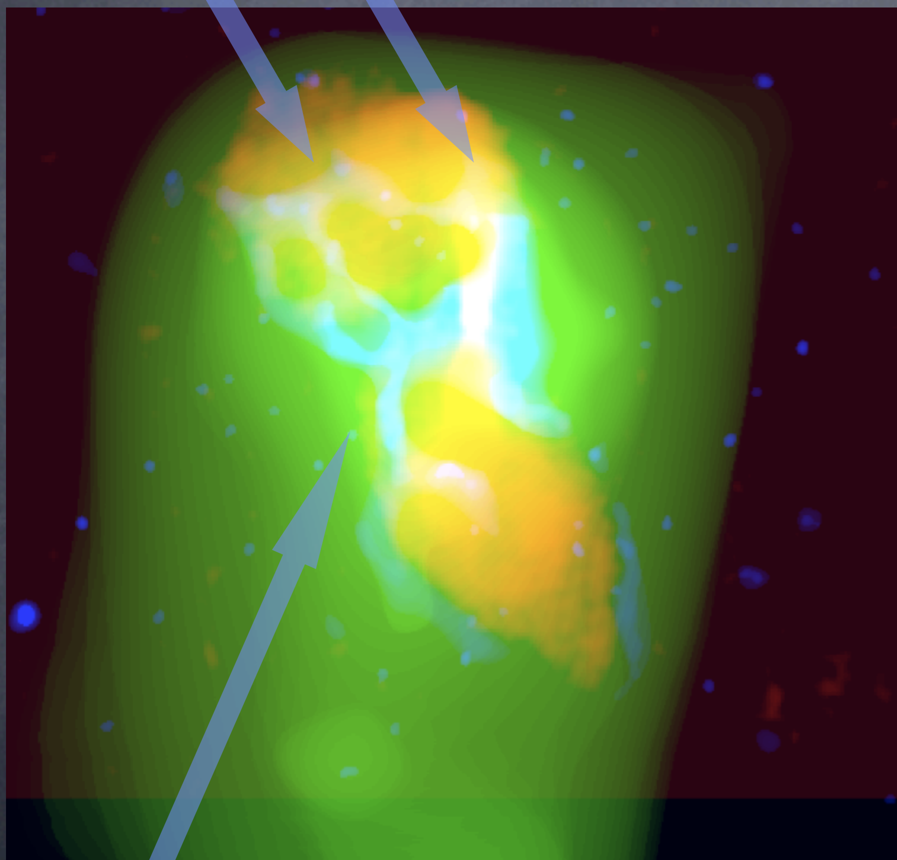

Orange - nonthermal
(radio) mission

Green - large scale
X-ray emission

Blue - small scale
X-ray emission

cross-field cosmic ray escape ?

Finoguenov, Ruszkowski, Jones, Bruggen, Vikhlinin, Mandell 2008

Ratio of the observed pressure and entropy to their mean profiles

First application of Voronoi tessellation method to *Chandra* data

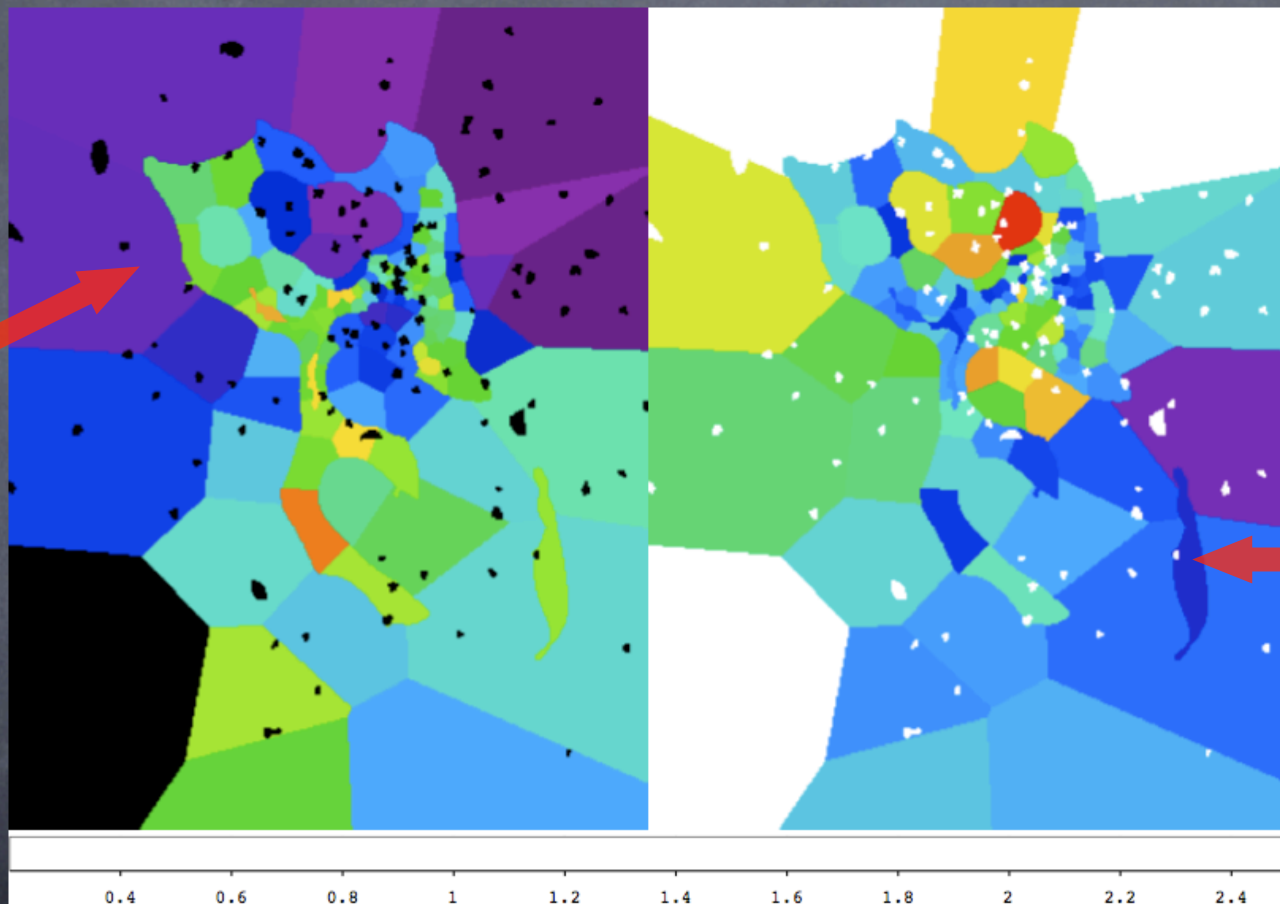

overpressured walls/waves

mildly supersonic expanssion

low entropy, entrainment

pressure

entropy

Synthetic "M84" replica !!

"Russian doll" bubble

Before

After

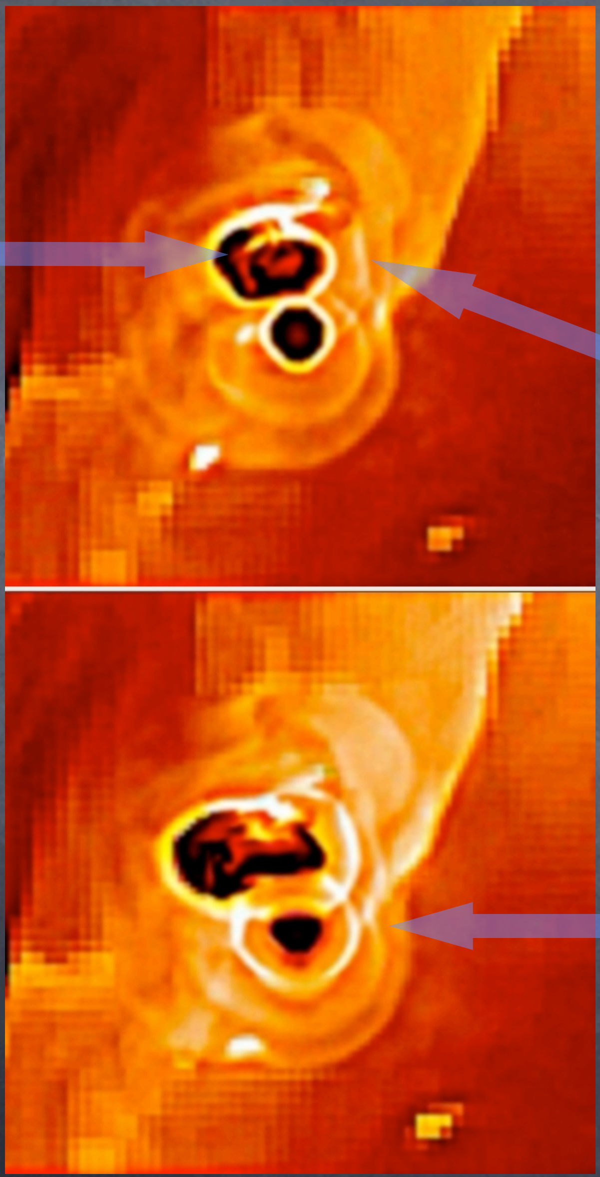

FLASH code AMR simulation of AGN feedback

Bruggen, Ruszkowski, Hallman 2005

bubble distorted by the relative AGN-ISM motion

waves detach from the bubble

and dissipate via transport processes

M84 energetics

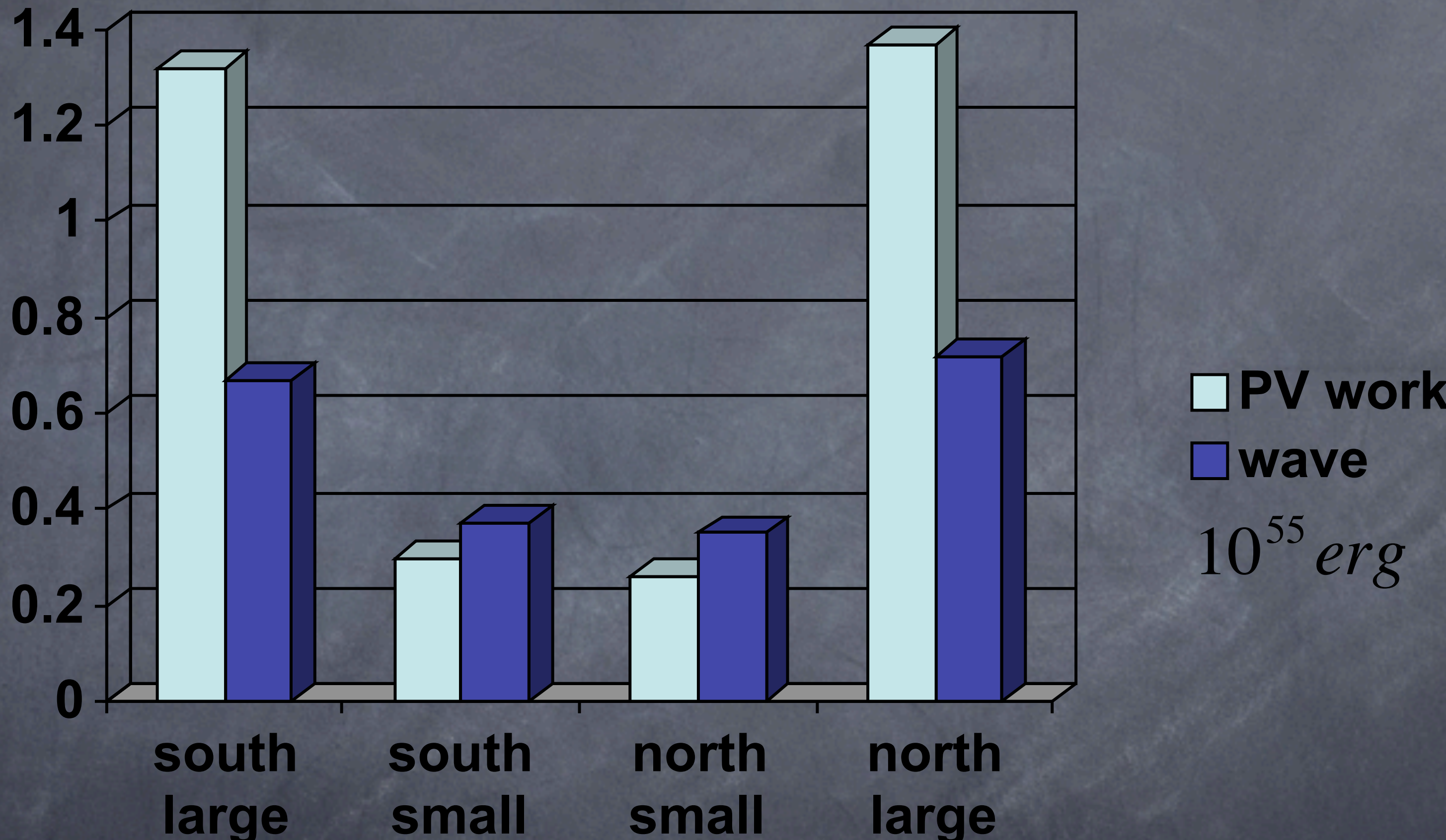

- wave-to-bubble ratio decreases with the distance
- significant energy in the waves

Magnetic fields in the ICM

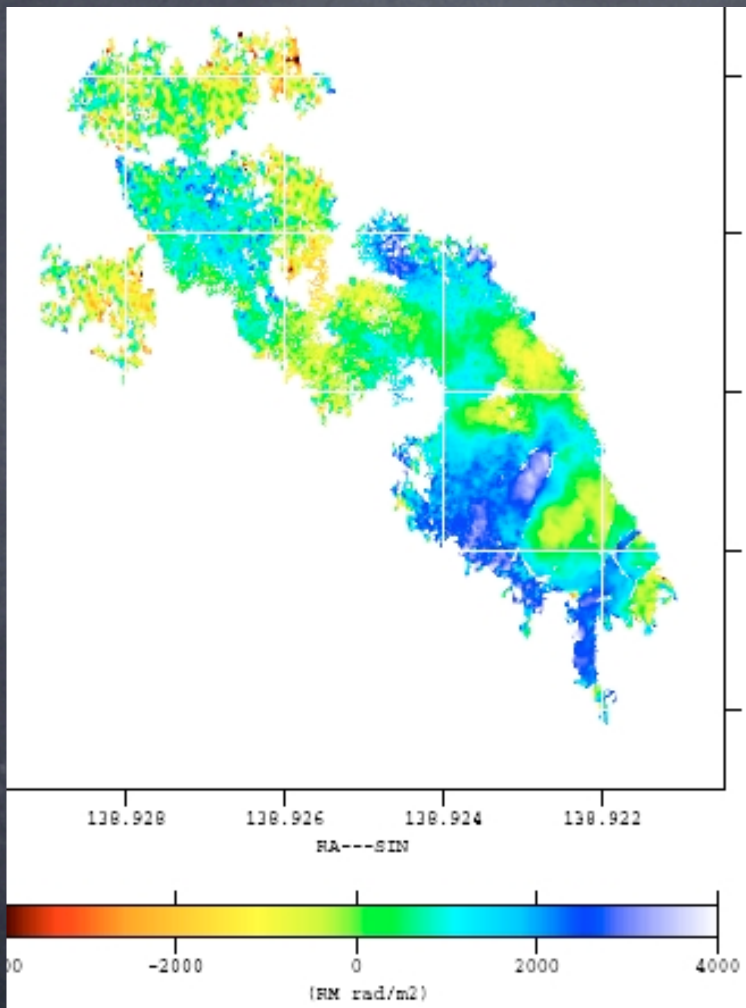

rotation measure map

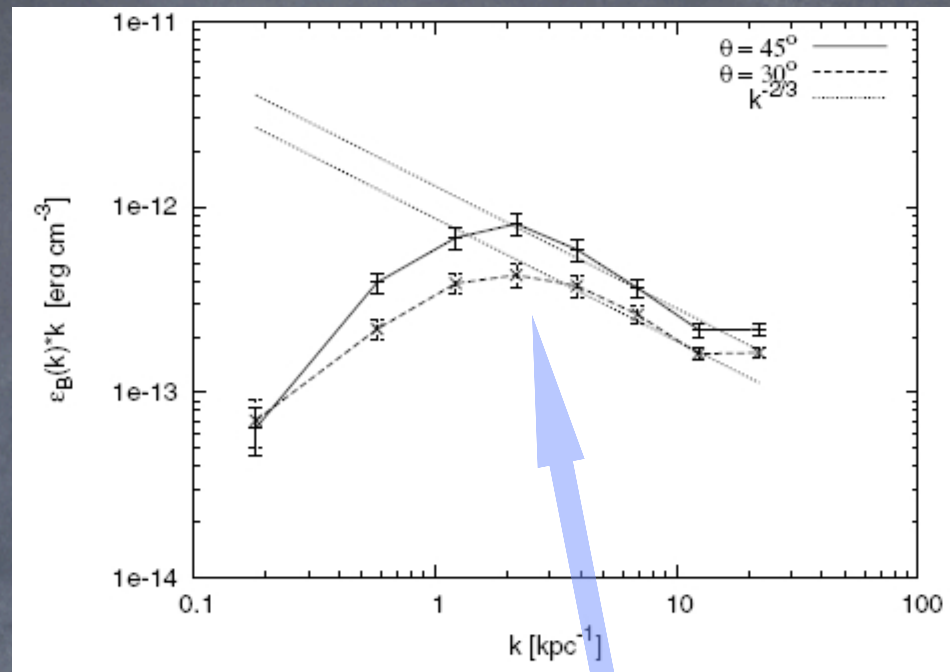

Power spectrum of B-field fluctuations (Ensslin & Vogt 2005)

Maximum near bubble size !

→ **magnetic draping**

3D MHD simulations with the *PENCIL* code

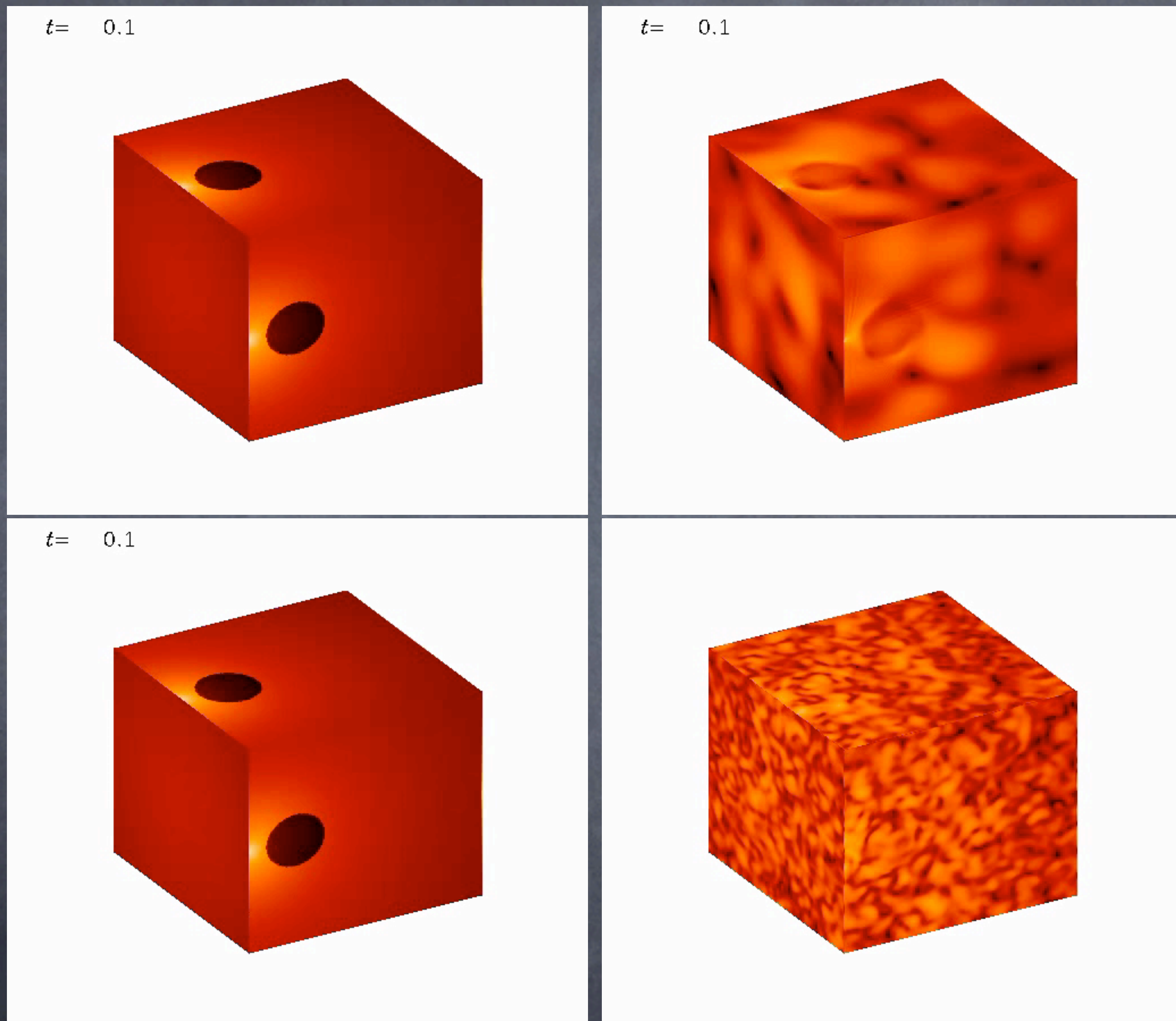

Ruszkowski, Ensslin, Bruggen, Heinz, Pfrommer 2007

Modes of escape of non-thermal particles from the bubbles

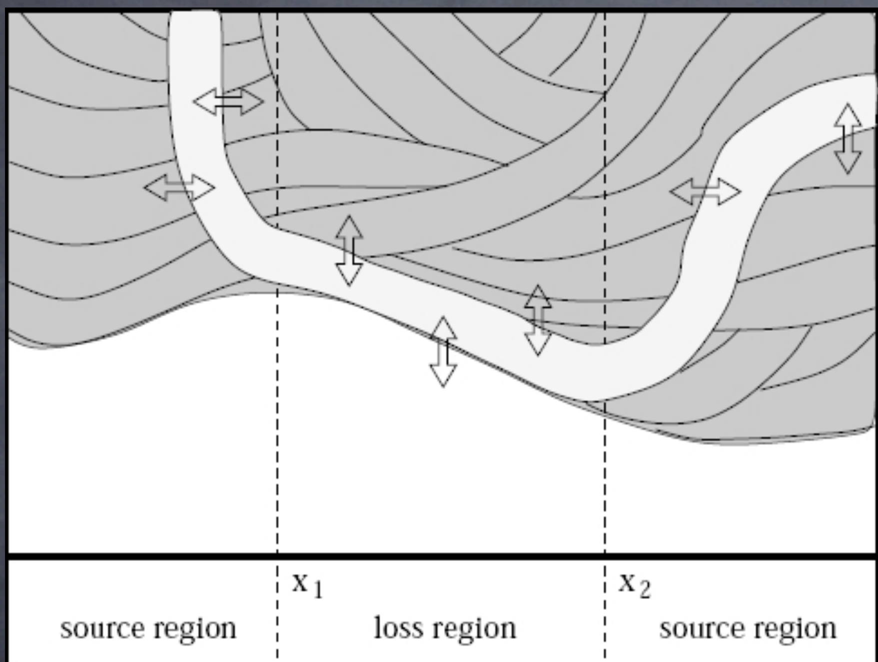

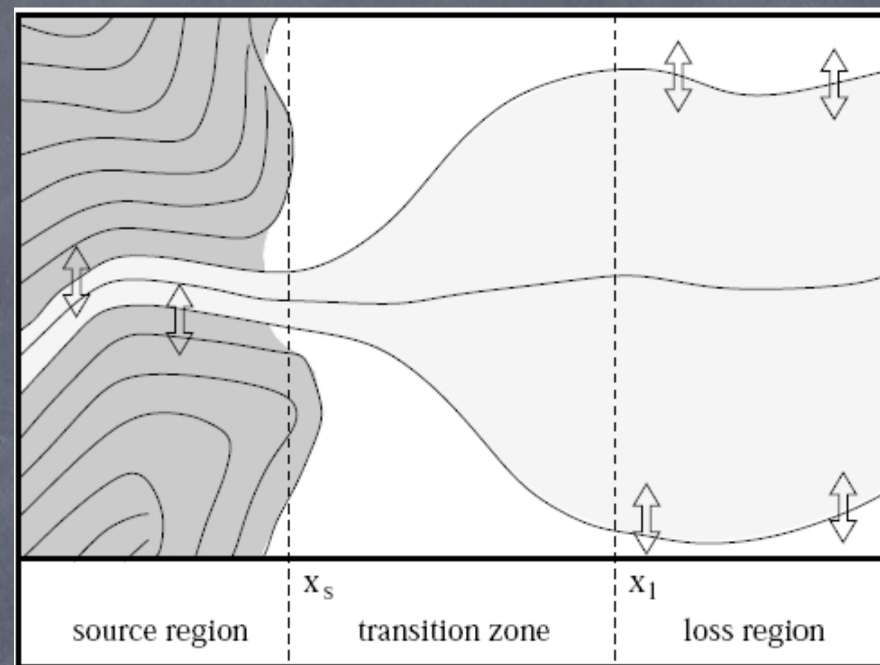

Cross-field diffusion
(recall M84)

Interface B-flux tubes
(e.g., in the bubble wakes
or due to
"piercing" by the jet - recall M84)

$$K_{perp} << K_{para}$$

Theoretical suggestion (Ensslin 2003)

$$K_{para} \sim 2 \times 10^{29} E_{10}^{1/3} r_5^{2/3} B_1^{-1/3} \eta^{-1} \text{ cm}^2\text{s}^{-1}$$

Observationally-based suggestion (Mathews & Brighenti 2007)

$$K \sim 7.5 \times 10^{29} r_5^2 / t_7 \text{ cm}^2\text{s}^{-1}$$

3D MHD simulations of

anisotropic particle escape

from the bubbles

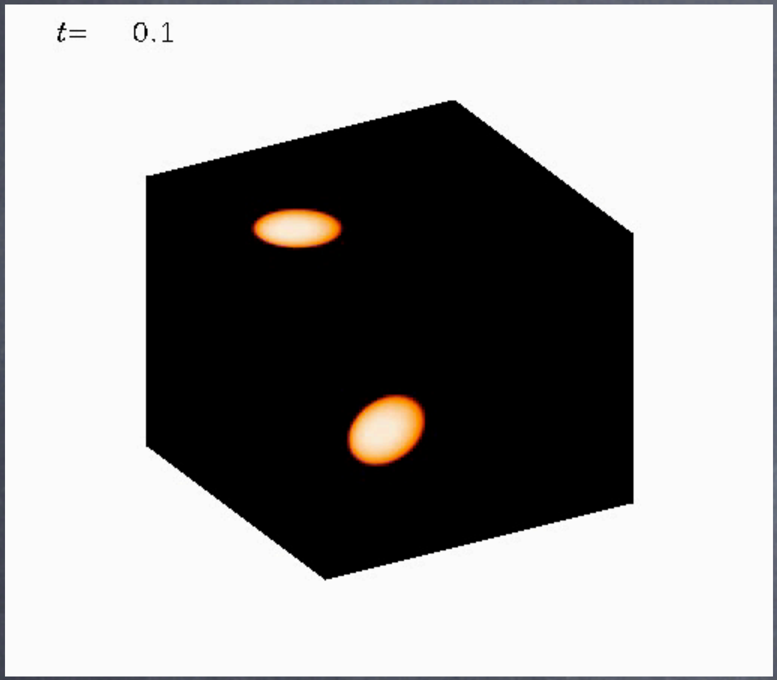

isotropic

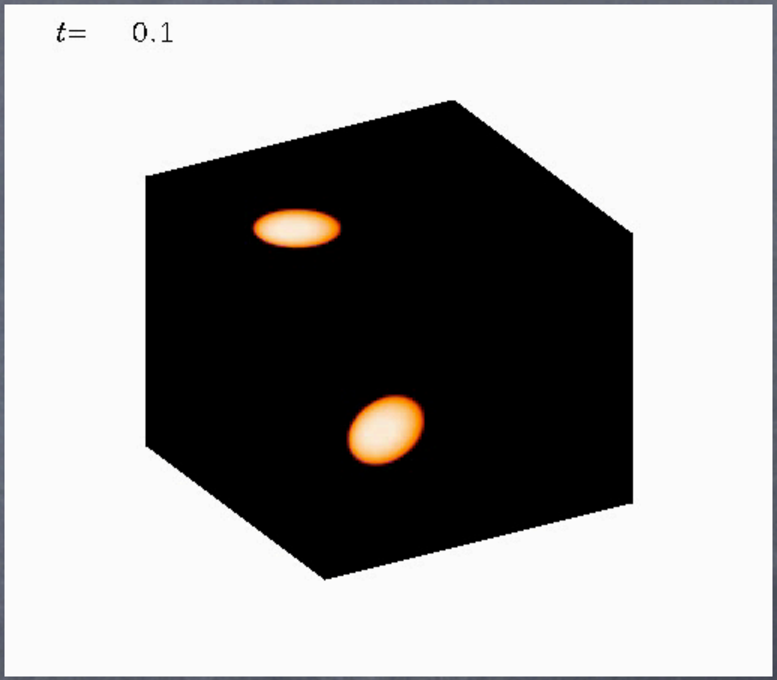

anisotropic

Ruszkowski, Ensslin, Bruggen, Begelman, Churazov 2008

Escape of non-thermal particles from the AGN bubbles

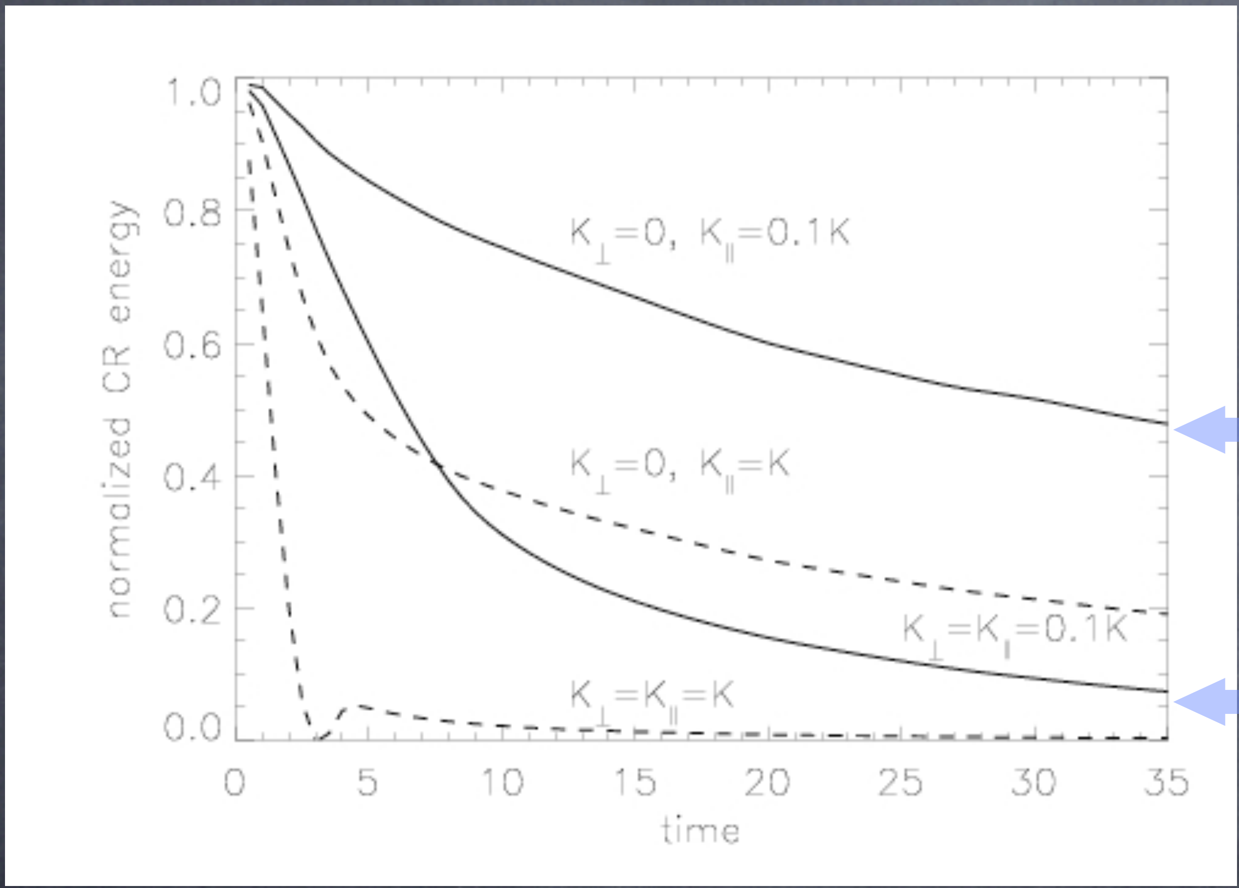

50% of non-thermal
Particles escape

Isotropic case
most particles escape

Ruszkowski, Ensslin, Bruggen, Begelman, Churazov 2008

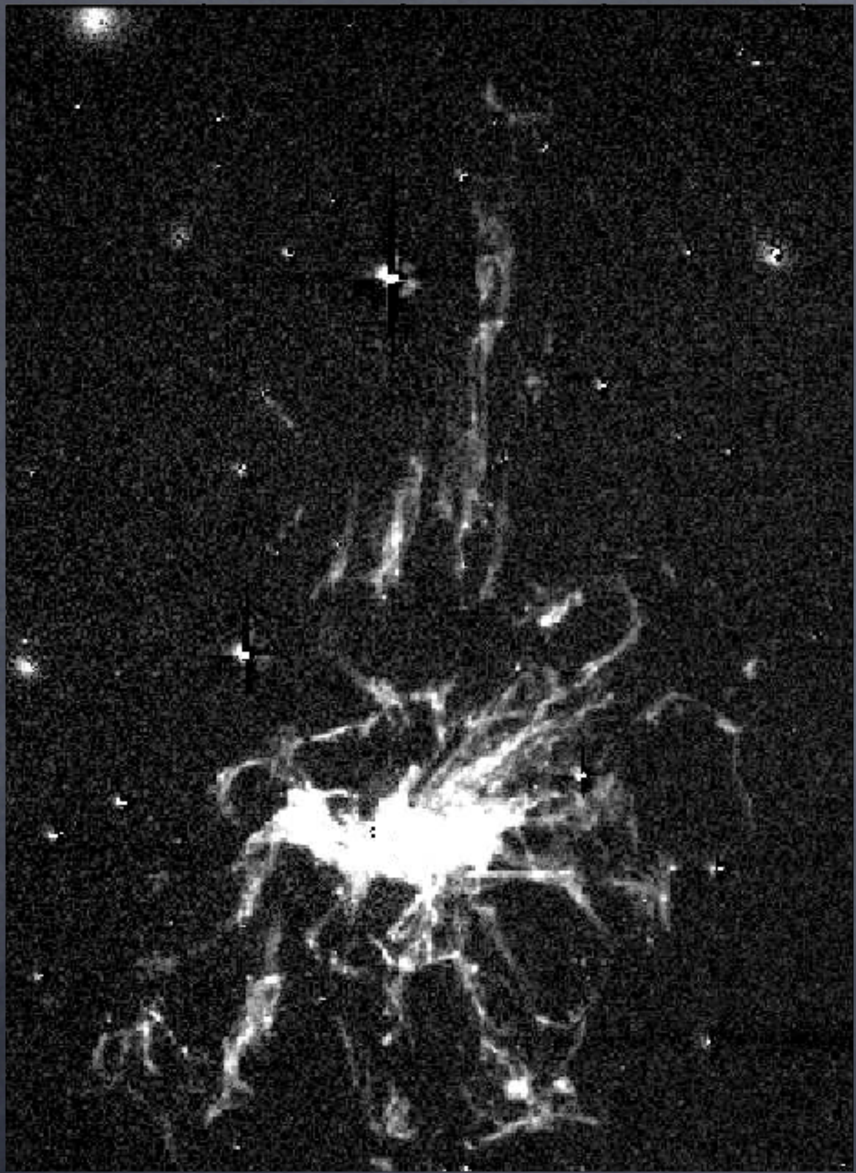

H_α **excitation**

X-rays from ICM ?
Fabian et al. 2003

Star clusters ?

Hatch et al. 2006

Conduction ?
Donahue et al. 2000

or

Cosmic ray heating ?
Diffusion in the bubble wake
Ruszkowski et al. 2008
Ferland et al. 2008 (w/ *CLOUDY*)

escape of CR from cluster centers
via the instability driven by
anisotropic
energy transport

$$\frac{d\Omega}{dr} < 0$$ classical MRI

$$\frac{dp_{cr}}{dr} < 0$$

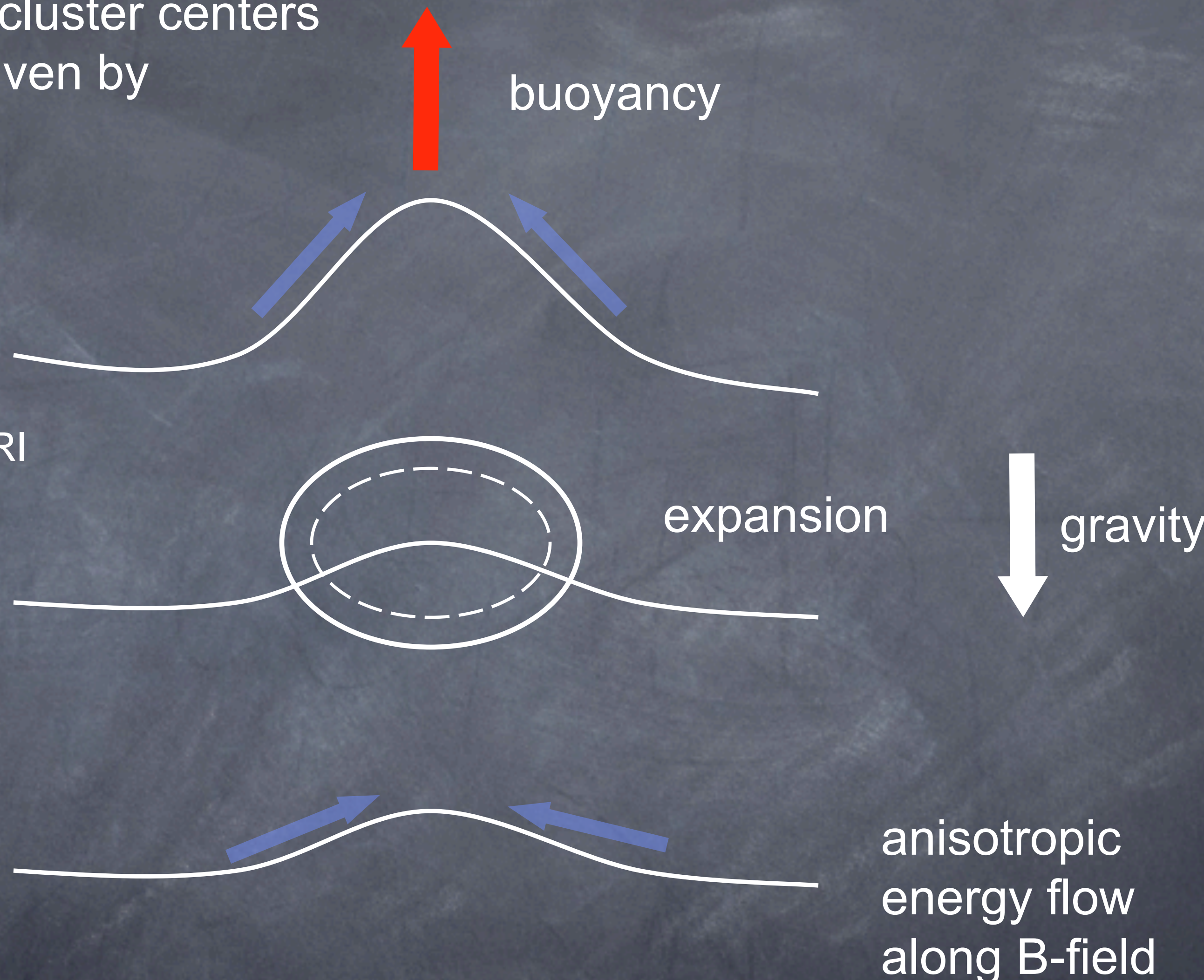

Perrish & Stone 2005
Chandran 2001
Ruszkowski & Parrish 2008, in prep.

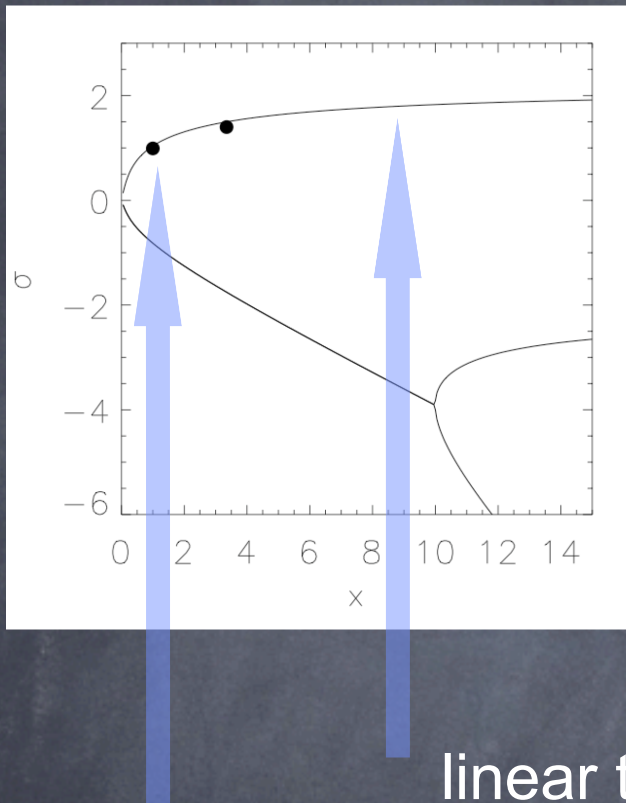

$$\text{perturbation} \propto e^{\sigma t}$$

$$x \propto K_{\parallel} k^2$$

$$t_{grow} \sim \sigma^{-1} \sim t_{dynamical}$$

linear theory

***PENCIL* code results**

Ruszkowski & Parrish 2008, in prep.

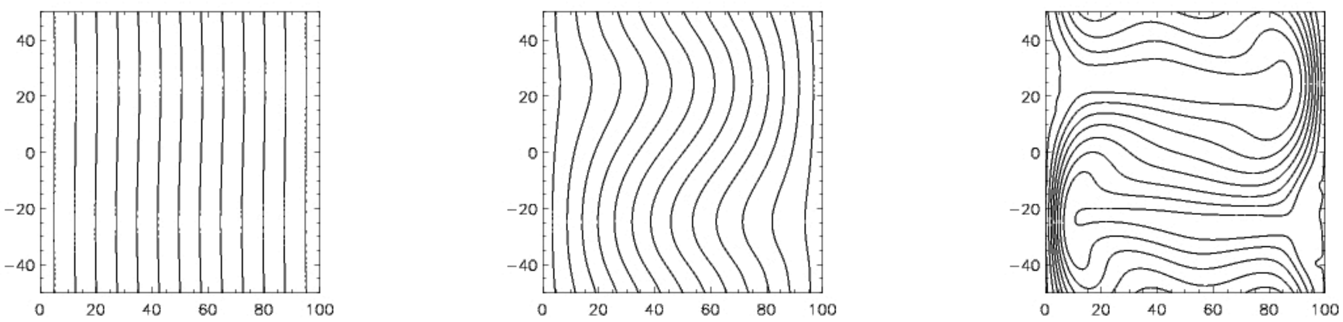

Figure 1: A snapshot from the *PENCIL* code tests of the development of the instability due to the anisotropy introduced by the magnetic field. This figure shows the evolution of the magnetic field lines subject to this instability. Gravity points in the $-x$ direction and the time increases from the left to the right panel.

the instability develops on the dynamical timescale

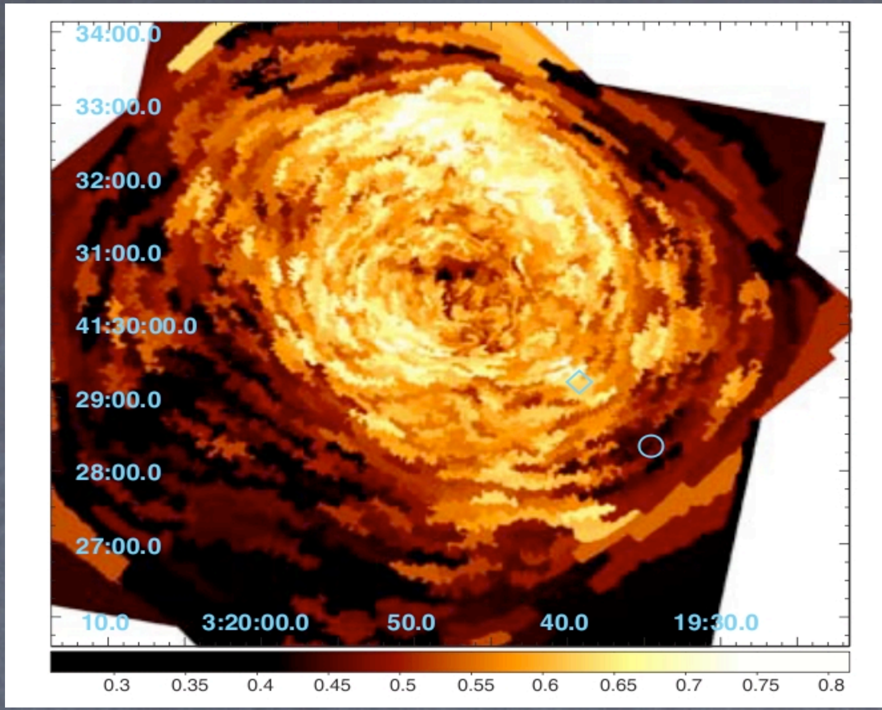

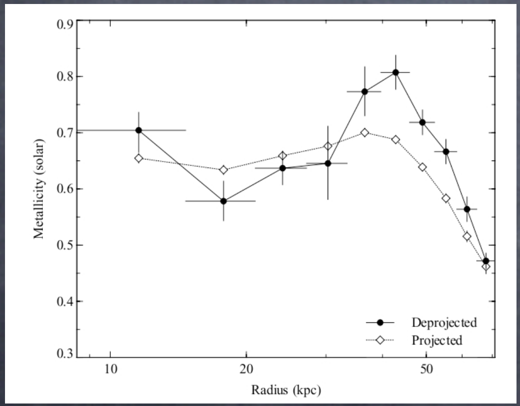

Perseus (Sanders & Fabian 2007)

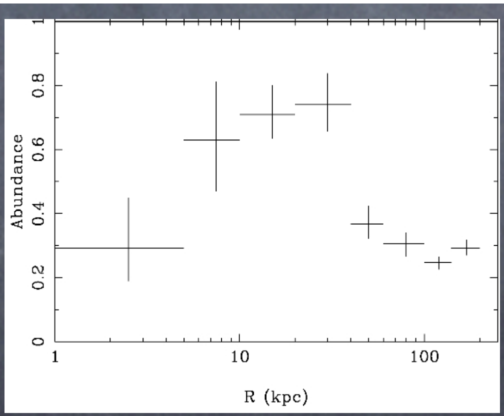

A2199 (Johnstone et al. 2002)

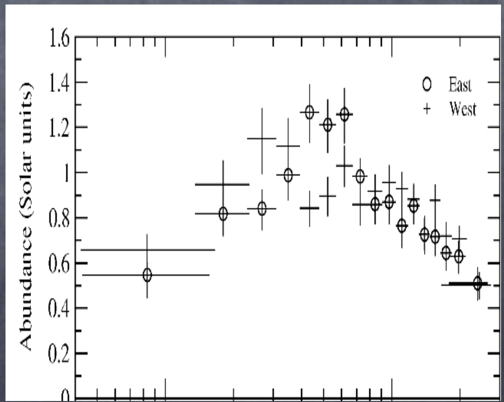

Centaurus (Sanders & Fabian 2002)

Gas overturn due to the convective instability ?

Summary

- ✓ **cool core - non cool core bimodality**
  - explained in a semianalytical study of global stability of clusters
  - cool core stabilized by AGN, non-cool core by conduction
  - no fine-tuning is required
- ✓ **M84 as an example of AGN feedback**
  - significant energy in waves
  - evidence for the escape of non-thermal particles from the AGN bubbles
- ✓ **Simulations with B-fields**
  - magnetic draping can efficiently prevent bubbles from disruption even for very weak magnetic fields
- ✓ **Simulations with anisotropic CR leakage**
  - difficult to confine all CRs in bubbles
  - CR can provide the excitation mechanism for the filaments
- ✓ **Simulations of plasma instabilities**
  - non-thermal particles can escape cluster centers on a dynamical timescale

  turbulent heating, metallicity profiles

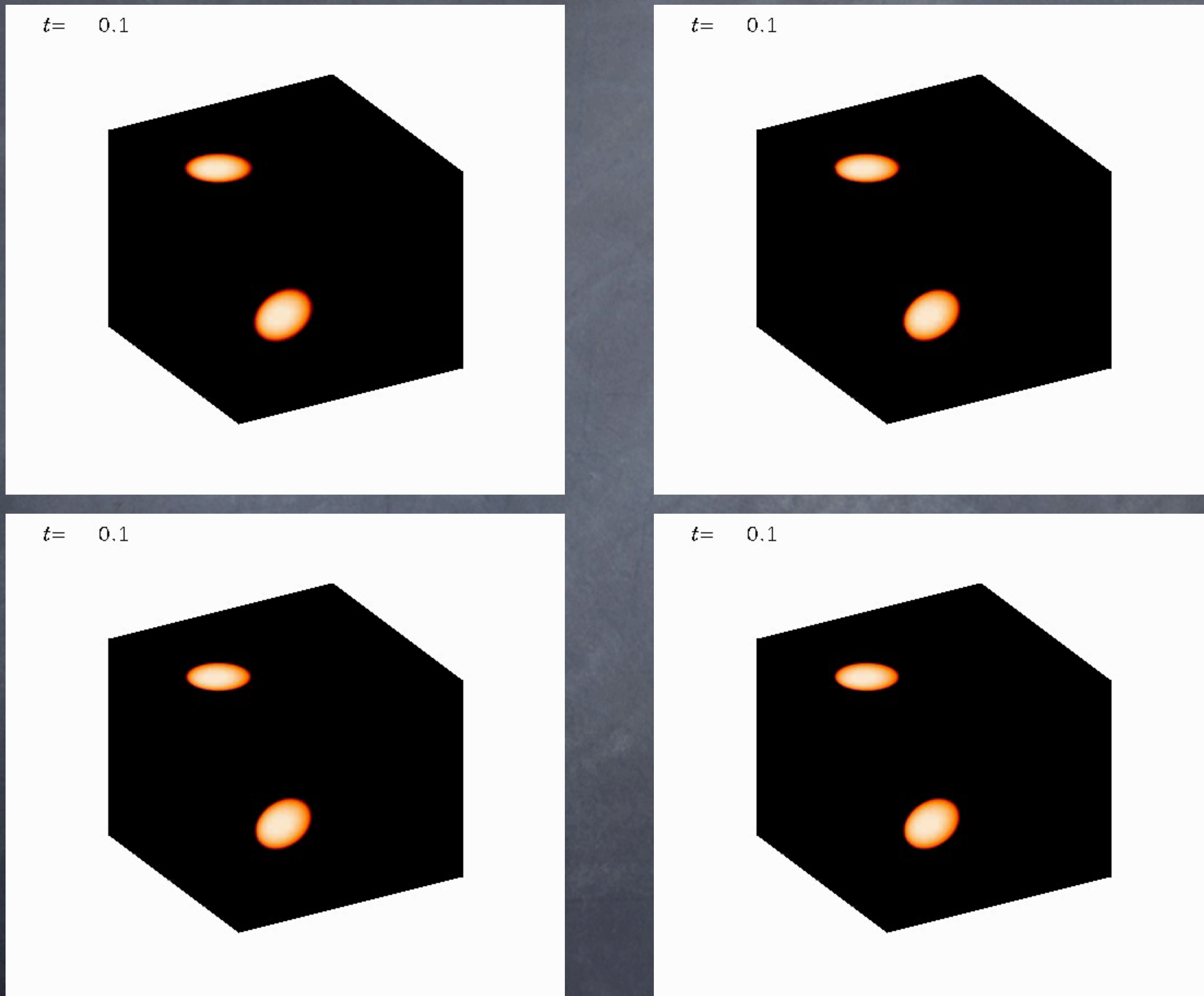
t= 0.1
t= 0.1
t= 0.1
t= 0.1

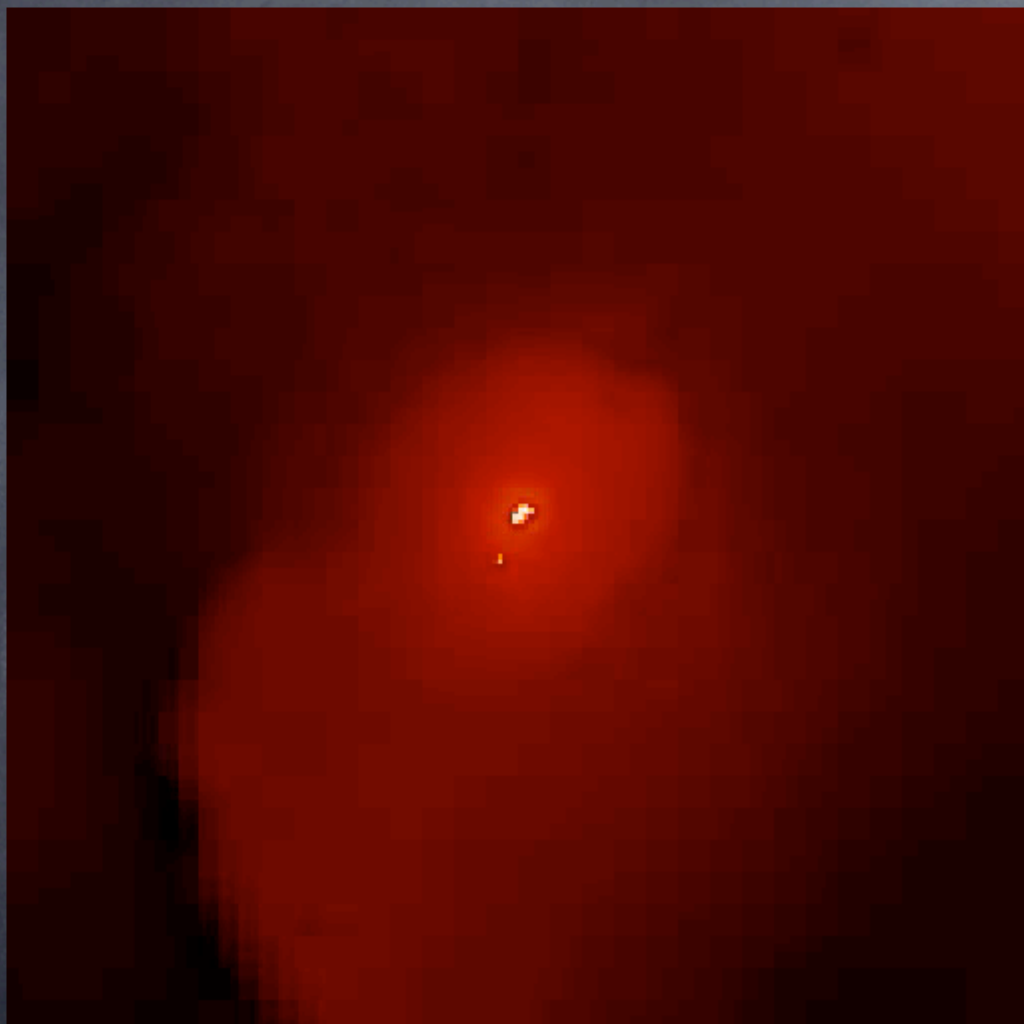

Table 2. Physical k/f values.

Cluster	Lobe[a]	Pressure ($\mathrm{eV\,cm^{-3}}$)	Re	Viscosity[b] ($10^{27}\ \mathrm{cm^2\,s^{-1}}$)	Energy[c] (10^{58} erg)	$k/f_{\rm eq}$	$k/f_{\rm sound}$[d]	$k/f_{\rm buoyancy}$	$k/f_{\rm refill}$
				Active bubbles					
3C401	N, R	39.6	1938	7.75	3.36	1.72	$0.51^{0.80}_{0.32}$	$1.60^{2.51}_{1.00}$	$0.62^{0.98}_{0.39}$
	S, R	31.9	1990	7.96	2.44	0.65	$0.22^{0.35}_{0.13}$	$0.57^{0.91}_{0.35}$	$0.29^{0.47}_{0.18}$
4C55.16	N, R	320	879	3.54	14.4	776	$93.5^{692}_{3.82}$	$90.4^{669}_{3.69}$	$52.4^{388}_{2.14}$
	S, R	277	1227	4.91	19.7	364	$32.8^{115}_{7.08}$	$47.0^{165}_{10.2}$	$24.4^{85.7}_{5.28}$
A262	E, R	55.4	301	1.20	0.040	352	221^{419}_{107}	528^{1003}_{257}	319^{605}_{155}
	W, R	55.4	330	1.32	0.041	308	$199^{396}_{94.0}$	387^{769}_{183}	300^{595}_{141}
A478	NE, R	440	471	1.88	0.092	177	$70.3^{152}_{31.4}$	225^{485}_{100}	$149^{321}_{66.5}$
	SW, R	440	585	2.34	0.34	653	$171^{368}_{76.2}$	885^{1909}_{395}	307^{661}_{137}
A1795	NW, R	356	190	0.76	0.28	107	$31.6^{43.0}_{22.6}$	$63.4^{86.3}_{42.5}$	$18.1^{24.6}_{13.0}$
	S, R	356	191	0.76	0.26	88.4	$22.3^{30.4}_{16.0}$	$39.8^{54.2}_{28.6}$	$14.2^{19.3}_{10.5}$
A2029	NW, R	669	153	0.61	0.44	33.1	$4.27^{32.5}_{0.49}$	$4.46^{33.9}_{0.51}$	$2.31^{17.6}_{0.26}$
	SE, R	669	170	0.68	0.71	45.8	$6.57^{50.0}_{0.75}$	$5.86^{44.7}_{0.67}$	$2.96^{22.5}_{0.34}$
M87	E-CJ, R	704	106	0.42	0.040	26.8	$8.75^{31.0}_{1.87}$	$28.6^{102}_{6.13}$	$8.53^{30.3}_{1.83}$
NGC 4472	E, R	106	83	0.33	0.011	4807	3531^{5010}_{2448}	5143^{7296}_{3565}	3209^{4553}_{2225}
	W, R	134	115	0.45	0.016	8727	5323^{7552}_{3690}	11401^{16175}_{7903}	5998^{8509}_{4158}
NGC 4636	NE, R	145	12.6	0.051	1.6×10^{-4}	61.5	$88.4^{237}_{28.3}$	$53.2^{142}_{17.0}$	$77.7^{208}_{24.9}$
	SW, R	145	12.4	0.050	1.1×10^{-4}	71.0	$95.9^{257}_{30.7}$	$19.4^{52.0}_{6.22}$	$94.4^{253}_{30.2}$
				Ghost bubbles					
A85	N, X	363	758	3.03	1.86	19462	4631^{28513}_{581}	6781^{41756}_{851}	4390^{27030}_{551}
	S, X	264	802	3.21	2.46	40635	10154^{62521}_{1275}	9936^{61178}_{1247}	8315^{51201}_{1044}
A2597	NE, X	242	604	2.41	2.3	268109	50559^{235504}_{7361}	55871^{260247}_{8134}	40104^{186808}_{5839}
	SW, X	253	801	3.20	3.6	445843	54361^{253218}_{7914}	86847^{404538}_{12644}	55729^{259589}_{8113}
Centaurus	N,X	99	58.6	0.23	0.062	152.7	$97.5^{128.8}_{73.4}$	$50.7^{67.0}_{38.2}$	$25.1^{33.2}_{18.9}$
Perseus ghost	W, X	232	242	9.70	3.0	16522	8771^{34615}_{1294}	976^{3853}_{144}	1355^{5347}_{200}
	S, X	206	381	1.52	4.1	17254	5174^{20419}_{763}	1176^{4641}_{173}	1339^{5285}_{198}
Perseus halo	SW, R	172	894	3.58	14.5	49178	7214^{7397}_{5859}	2744^{2814}_{2229}	3024^{3101}_{2456}
RBS797	W, X	1848	1353	5.41	29.2	920472	20118^{126028}_{2482}	19438^{121768}_{2398}	10313^{64603}_{1272}
	E, X	1848	1353	5.41	29.2	920472	20118^{126028}_{2482}	19438^{121768}_{2398}	10313^{64603}_{1272}

Notes. [a]The codes for the lobes are: N, northern; S, southern; E, eastern; W, western etc.; X, sizes from X-ray image; R, sizes from radio image; CJ, counter jet cavity in M87. [b]The viscosity is estimated assuming that the flow is laminar and has a Reynolds number of 1000. [c]The energy quoted here is $E = PV$, so the values have to be multiplied by the appropriate $\gamma/(\gamma - 1)$. [d]The range on the limits on k/f from the uncertainty in the spectral index are given by the maximum values (superscript) and minimum values (subscript). The uncertainties from other parameters are shown in Fig. 1.

Dunn & Fabian 2005

System	$pV_{\rm tot}$ (10^{58} ergs)	$P_{\rm cav,\,tot}$[a] (10^{42} ergs $\mathrm{s^{-1}}$)	$L_{\rm X}$[b] (10^{42} ergs $\mathrm{s^{-1}}$)
A85	$1.2^{+1.2}_{-0.4}$	37^{+37}_{-11}	365 ± 20
A133	24^{+11}_{-1}	620^{+260}_{-20}	106 ± 2
A262	$0.13^{+0.10}_{-0.03}$	$9.7^{+7.5}_{-2.6}$	$11.1^{+0.4}_{-0.3}$
Perseus	19^{+20}_{-5}	150^{+100}_{-30}	554 ± 2
2A 0335+096	$1.1^{+1.0}_{-0.3}$	24^{+23}_{-6}	338 ± 2
A478	$1.5^{+1.1}_{-0.4}$	100^{+80}_{-20}	1440 ± 10
MS 0735.6+7421	1600^{+1700}_{-600}	6900^{+7600}_{-2600}	450 ± 10
PKS 0745-191	69^{+56}_{-10}	1700^{+1400}_{-300}	2300 ± 30
4C 55.16	12^{+12}_{-4}	420^{+440}_{-160}	640 ± 20
Hydra A	64^{+48}_{-11}	430^{+200}_{-50}	282 ± 2
RBS 797	38^{+50}_{-15}	1200^{+1700}_{-500}	3100^{+100}_{-130}
Zw 2701	350^{+530}_{-200}	6000^{+8900}_{-3500}	430^{+20}_{-30}
Zw 3146	380^{+460}_{-110}	5800^{+6800}_{-1500}	3010^{+70}_{-90}
A1068	...	20[c]	...
M84	$0.003^{+0.005}_{-0.002}$	$1.0^{+1.5}_{-0.6}$	0.07 ± 0.01
M87	$0.020^{+0.014}_{-0.003}$	$6.0^{+4.2}_{-0.9}$	$8.30^{+0.03}_{-0.04}$
Centaurus	$0.060^{+0.051}_{-0.015}$	$7.4^{+5.8}_{-1.8}$	28.1 ± 0.3
HCG 62	$0.046^{+0.073}_{-0.028}$	$3.9^{+6.1}_{-2.3}$	1.8 ± 0.2
A1795	$4.7^{+6.6}_{-1.6}$	160^{+230}_{-50}	625^{+6}_{-11}
A1835	47^{+50}_{-16}	1800^{+1900}_{-600}	3160^{+60}_{-90}
PKS 1404-267	$0.12^{+0.15}_{-0.05}$	20^{+26}_{-9}	27 ± 1
MACS J1423.8+2404	29^{+52}_{-19}	1400^{+2500}_{-900}	2290 ± 30
A2029	$4.8^{+2.7}_{-0.1}$	87^{+49}_{-4}	1160 ± 10
A2052	$1.7^{+2.3}_{-0.7}$	150^{+200}_{-70}	97 ± 1
MKW 3S	38^{+39}_{-4}	410^{+420}_{-44}	104 ± 2
A2199	$7.5^{+6.6}_{-1.5}$	270^{+250}_{-60}	142 ± 1
Hercules A	31^{+40}_{-9}	310^{+400}_{-90}	210^{+10}_{-20}
3C 388	$5.2^{+7.5}_{-2.1}$	200^{+280}_{-80}	27^{+2}_{-3}
3C 401	11^{+20}_{-7}	650^{+1200}_{-420}	37^{+2}_{-7}
Cygnus A	84^{+70}_{-14}	1300^{+1100}_{-200}	420 ± 4
Sersic 159/03	25^{+26}_{-8}	780^{+820}_{-260}	220 ± 6
A2597	$3.6^{+4.6}_{-1.5}$	67^{+87}_{-29}	470^{+8}_{-17}
A4059	$3.0^{+2.5}_{-0.9}$	96^{+89}_{-35}	93 ± 1

Rafferty et al. 2006

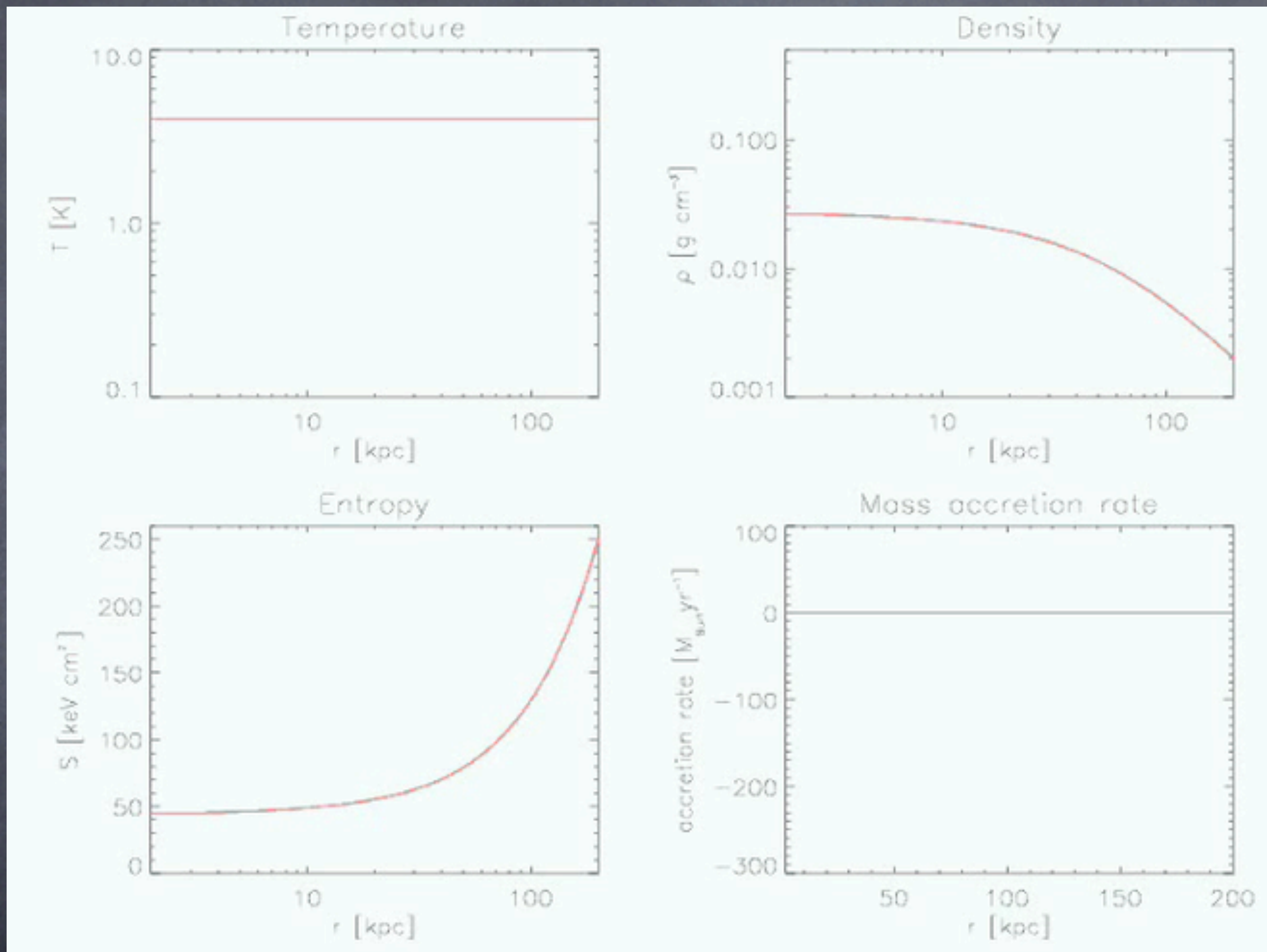

Temperature
10.0
1.0
0.1
T [K]
10
100
r [kpc]
Density
0.100
0.010
0.001
ρ [g cm⁻³]
10
100
r [kpc]
Entropy
250
200
150
100
50
0
S [keV cm²]
10
100
r [kpc]
Mass accretion rate
100
0
−100
−200
−300
accretion rate [M_sun yr⁻¹]
50
100
150
200
r [kpc]

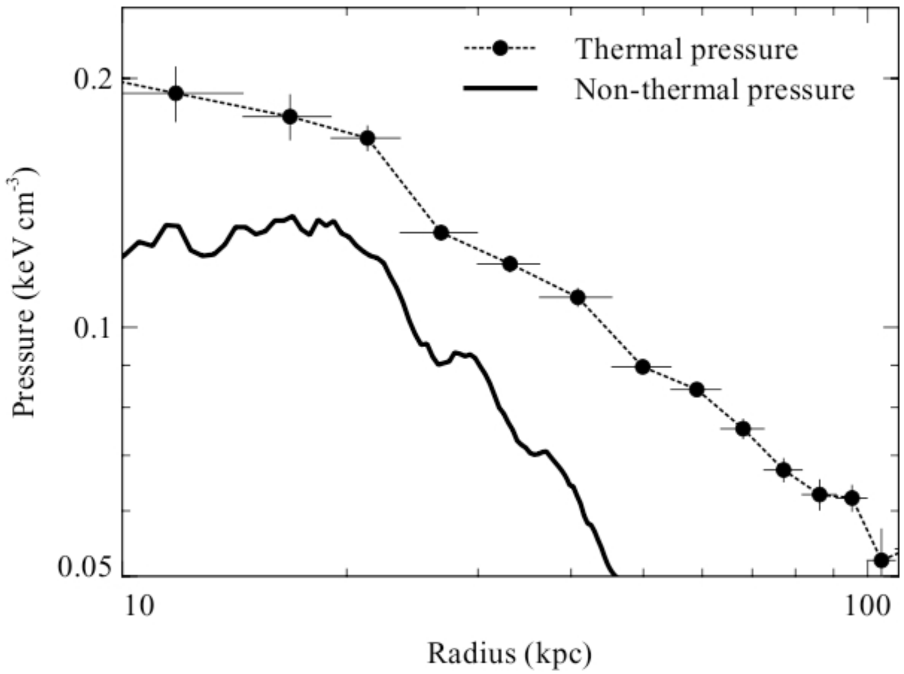

Figure 24. Inferred average non-thermal particle pressure calculated from the $\Gamma = 1.5$ power law plus multitemperature results in Fig. 21, assuming inverse Compton emission. Also plotted is the average thermal gas electron pressure from Sanders et al. (2004).

Sanders & Fabian 2007

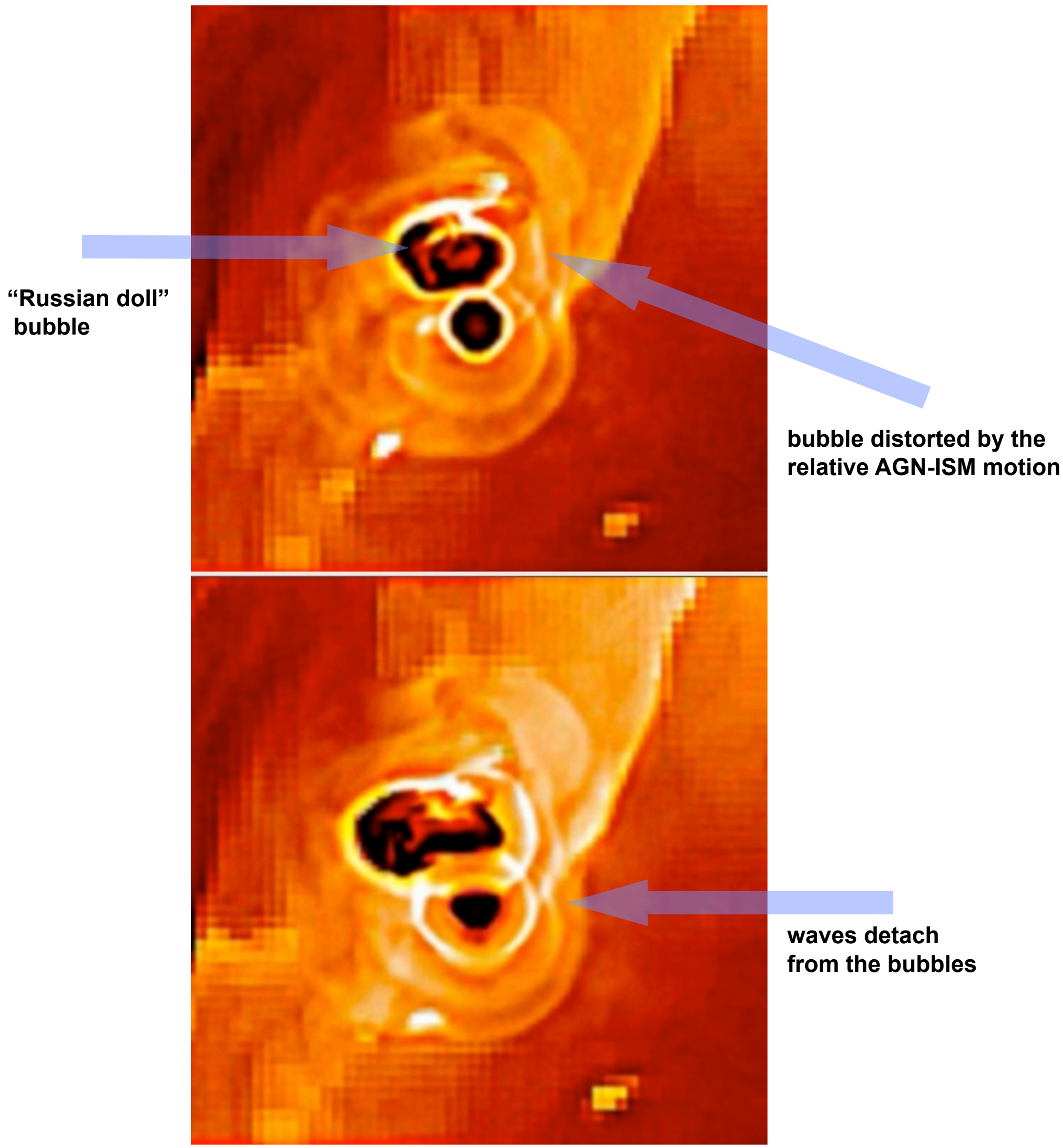
“Russian doll”
bubble
bubble distorted by the
relative AGN-ISM motion
waves detach
from the bubbles

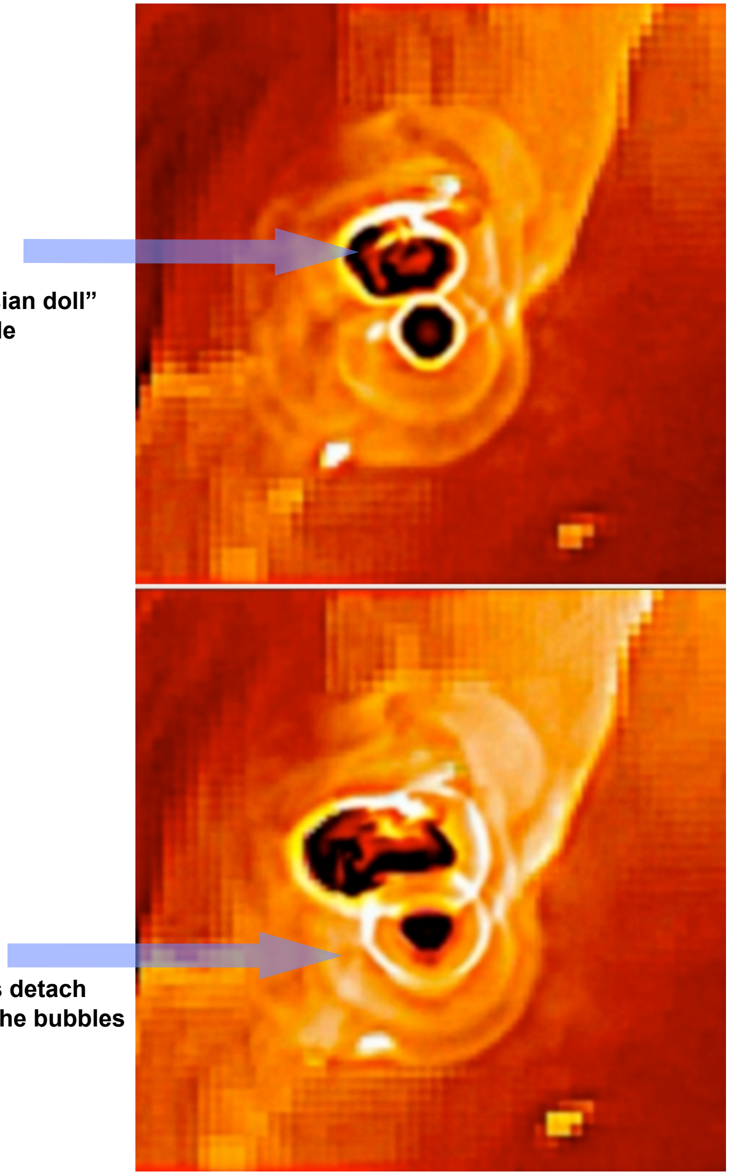

“Russian doll”
bubble
waves detach
from the bubbles